Title: On the modeling of black hole ringdown

Speakers: Naritaka Oshita

Series: Strong Gravity

Date: November 10, 2022 - 1:00 PM

URL: https://pirsa.org/22110054

Abstract: A gravitational wave from a binary black hole merger is an important probe to test gravity. Especially, the observation of ringdown may allow us to perform a robust test of gravity as it is a superposition of excited quasi-normal (QN) modes of a Kerr black hole. The excitation factor is an important quantity that quantifies the excitability of QN modes and is independent of the initial data of the black hole.

In this talk, I will show which QN modes can be important (i.e., have higher excitation factors) and will discuss how we can determine the start time of ringdown to maximally enhance the detectability of the QN modes.

Also, I will introduce my recent conjecture on the modeling of ringdown waveform:

the thermal ringdown model in which the ringdown of a small mass ratio merger involving a spinning black hole can be modeled by the Fermi-Dirac distribution.

Zoom link: https://pitp.zoom.us/j/96739417230?pwd=Tm00eHhxNzRaOEQvaGNzTE85Z1ZJdz09

Strong Gravity seminar @ Perimeter Institute, November 10th, 2022

On the modeling of black hole ringdown

Naritaka Oshita (RIKEN, iTHEMS)

RIKEN Interdisciplinary Theoretical and Mathematical Sciences Program

NO and D. Tsuna arXiv: 2210.14049
NO arXiv: 2208.02923
NO arXiv: 2109.09757

Quasi-Normal (QN) Modes of BHs and Ringdown

B. P. Abbott et al. (2016)

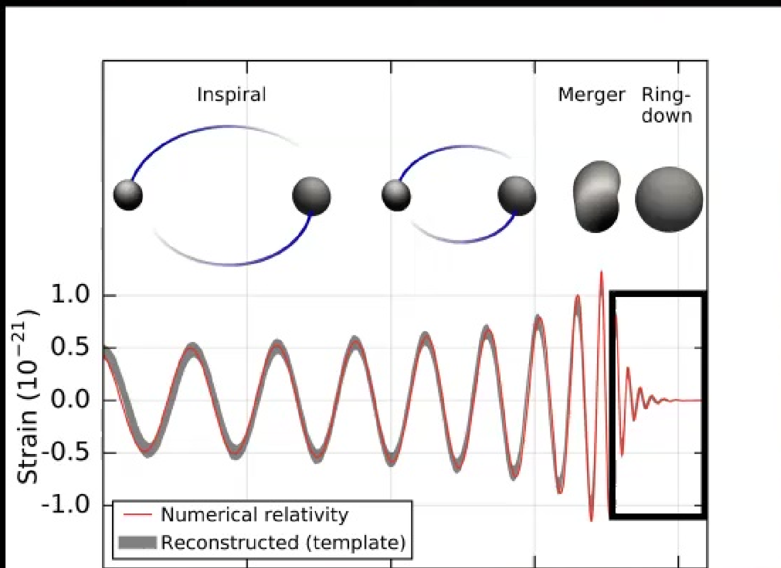

relaxation process of a BH
=ringdown phase
= superposition of quasi-normal modes

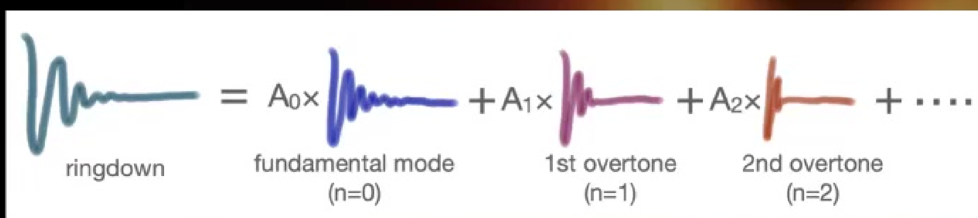

Credit: EHT collaboration

Quasi-Normal (QN) Modes of BHs and Ringdown

B. P. Abbott et al. (2016)

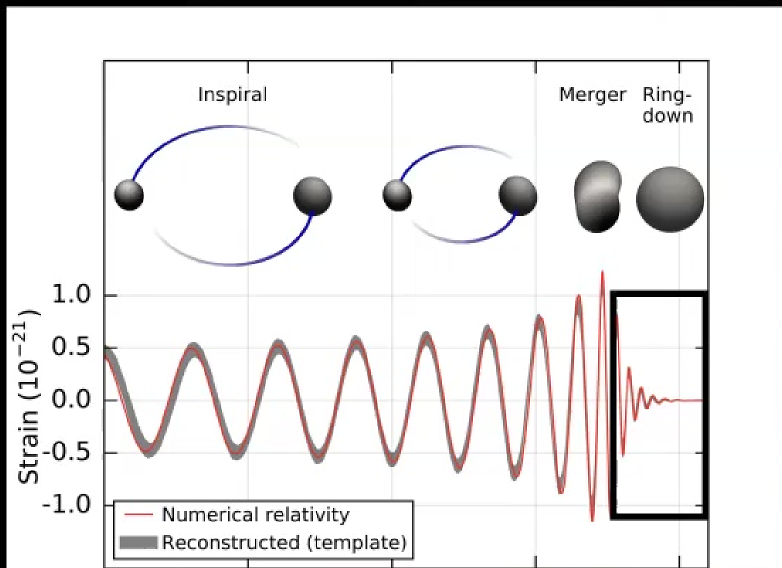

relaxation process of a BH
=ringdown phase
= superposition of quasi-normal modes

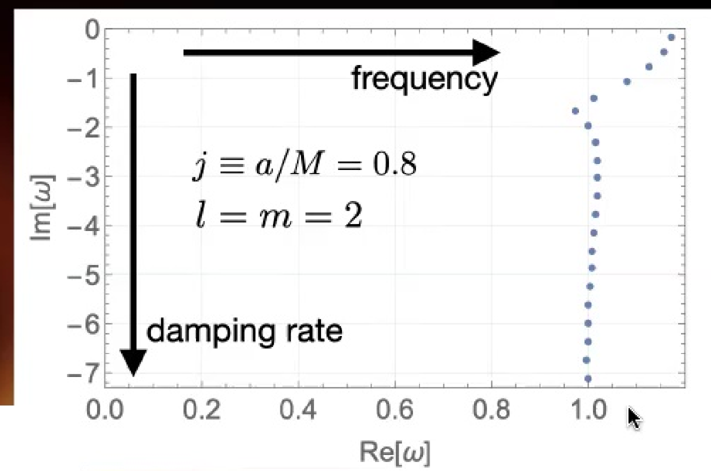

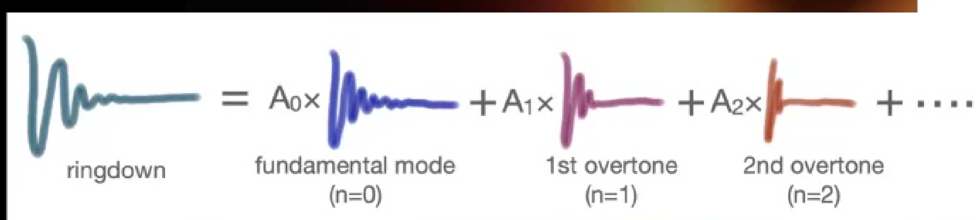

$$h_{\mathrm{ringdown}} \sim \sum_n A_n e^{-t/\tau_n} \cos[f_n(t - r^* - t_0) + \delta_n]$$

determined only by mass and angular momentum (no-hair theorem)

Credit: EHT collaboration

Why is a BH ringing important?

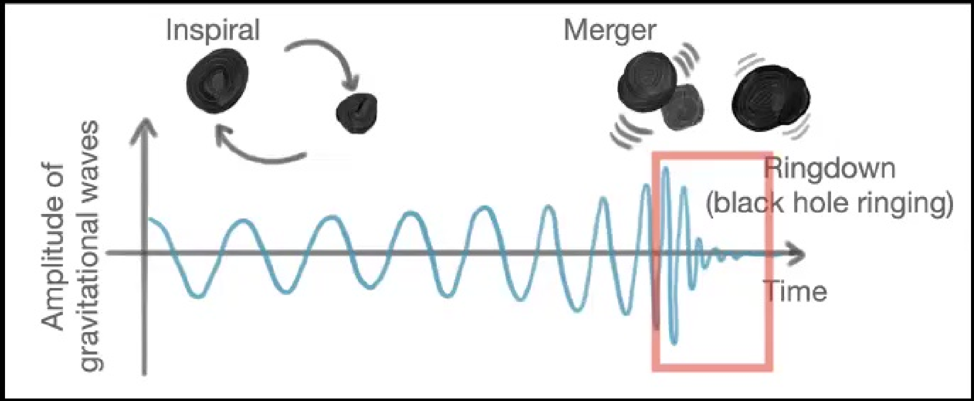

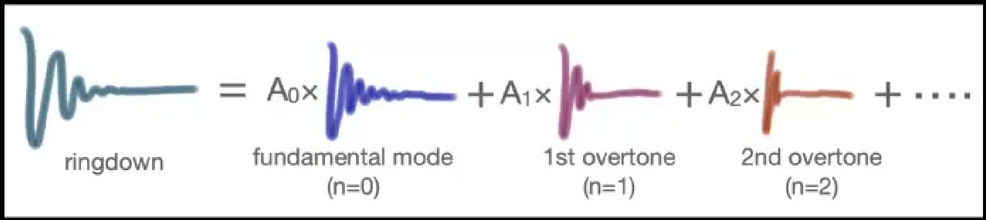

→ Measurement of each QN mode

→ Test of GR in strong-gravity regimes

Overtone QN modes

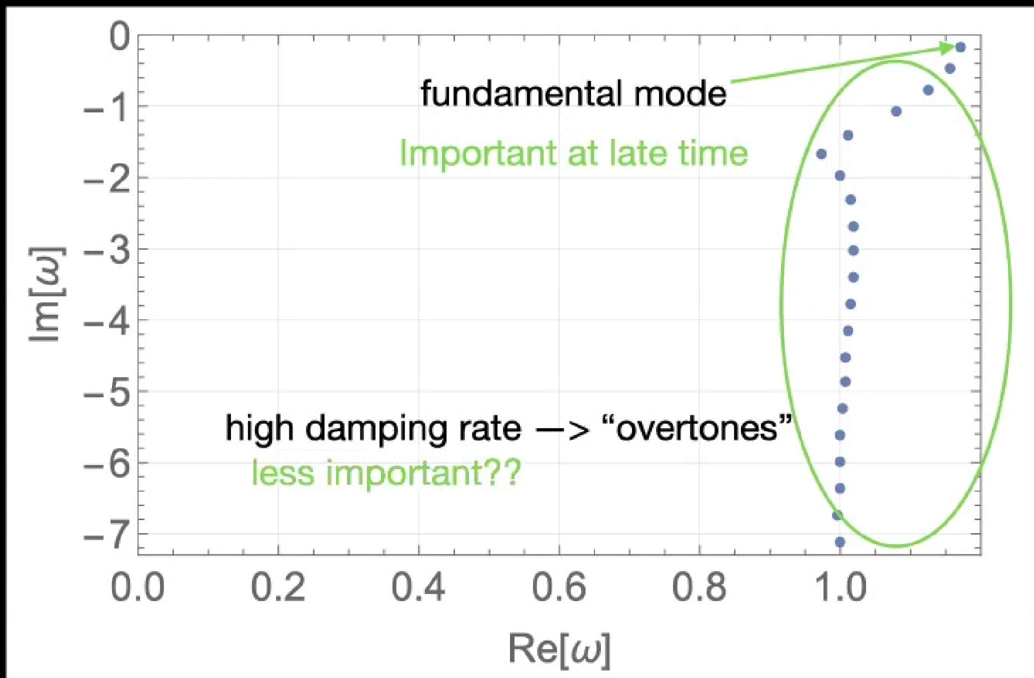

Kerr BH (j=0.8, M=0.5)

When does ringdown start?

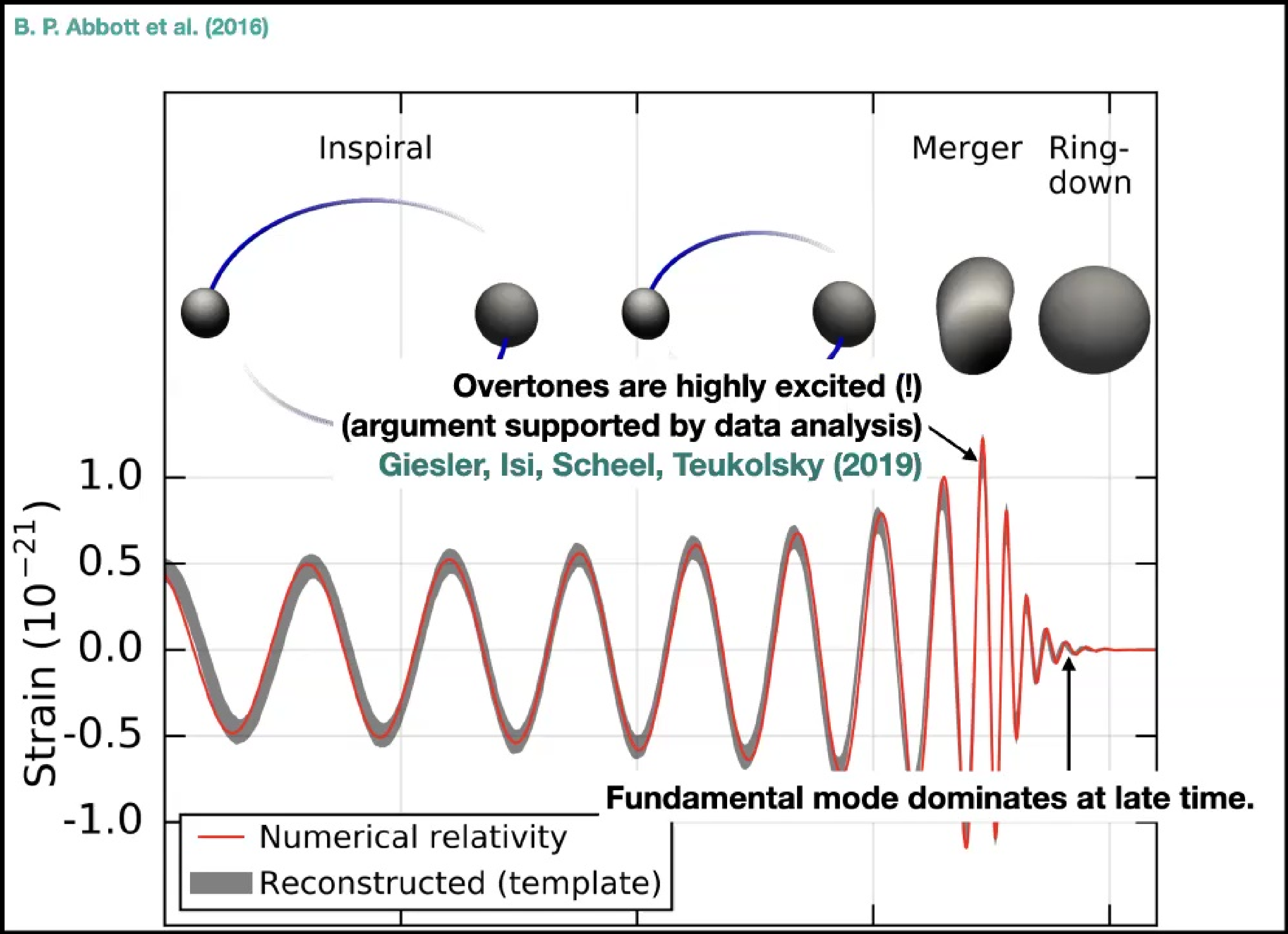

Binary Black Hole with the comparable mass ratio

Black hole ringdown: the importance of overtones

Matthew Giesler,[1,*] Maximiliano Isi,[2,3,†] Mark A. Scheel,[1] and Saul A. Teukolsky[1,4]

[1]TAPIR, Walter Burke Institute for Theoretical Physics, California Institute of Technology, Pasadena, CA 91125, USA
[2]LIGO Laboratory, Massachusetts Institute of Technology, Cambridge, Massachusetts 02139, USA
[3]LIGO Laboratory, California Institute of Technology, Pasadena, California 91125, USA
[4]Cornell Center for Astrophysics and Planetary Science, Cornell University, Ithaca, New York 14853,

(Dated: January 13, 2020)

It is possible to infer the mass and spin of the remnant black hole from binary black hole mergers by comparing the ringdown gravitational wave signal to results from studies of perturbed Kerr spacetimes. Typically these studies are based on the fundamental quasinormal mode of the dominant $\ell = m = 2$ harmonic. By modeling the ringdown of accurate numerical relativity simulations, we find, in agreement with previous findings, that the fundamental mode alone is insufficient to recover the true underlying mass and spin, unless the analysis is started very late in the ringdown. Including higher overtones associated with this $\ell = m = 2$ harmonic resolves this issue, and provides an unbiased estimate of the true remnant parameters. Further, including overtones allows for the modeling of the ringdown signal for all times beyond the peak strain amplitude, indicating that the linear quasinormal regime starts much sooner than previously expected. This implies that the spacetime is well described as a linearly perturbed black hole with a fixed mass and spin as early as the peak. A model for the ringdown beginning at the peak strain amplitude can exploit the higher signal-to-noise ratio in detectors, reducing uncertainties in the extracted remnant quantities. These results should be taken into consideration when testing the no-hair theorem.

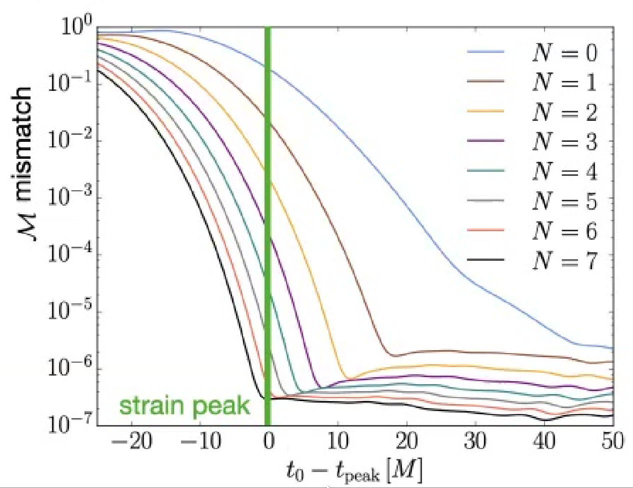

Giesler, Isi, Scheel, Teukolsky (2019)

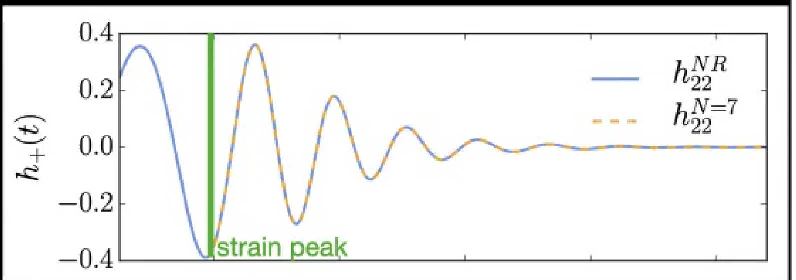

Fundamental mode ⟵⟶ Higher overtones

N	A_0	A_1	A_2	A_3	A_4	A_5	A_6	A_7	$t_{\rm fit} - t_{\rm peak}$
0	0.971	-	-	-	-	-	-	-	47.00
1	0.974	3.89	-	-	-	-	-	-	18.48
2	0.973	4.14	8.1	-	-	-	-	-	11.85
3	0.972	4.19	9.9	11.4	-	-	-	-	8.05
4	0.972	4.20	10.6	16.6	11.6	-	-	-	5.04
5	0.972	4.21	11.0	19.8	21.4	10.1	-	-	3.01
6	0.971	4.22	11.2	21.8	28	21	6.6	-	1.50
7	0.971	4.22	11.3	23.0	33	29	14	2.9	0.00

Binary Black Hole with the comparable mass ratio

Black hole ringdown: the importance of overtones

Matthew Giesler,[1,*] Maximiliano Isi,[2,3,†] Mark A. Scheel,[1] and Saul A. Teukolsky[1,4]

R, Walter Burke Institute for Theoretical Physics, California Institute of Technology, Pasadena, CA 91125, USA
[2]LIGO Laboratory, Massachusetts Institute of Technology, Cambridge, Massachusetts 02139, USA
[3]LIGO Laboratory, California Institute of Technology, Pasadena, California 91125, USA
Cornell Center for Astrophysics and Planetary Science, Cornell University, Ithaca, New York 14853,

(Dated: January 13, 2020)

It is possible to infer the mass and spin of the remnant black hole from binary black hole mergers by comparing the ringdown gravitational wave signal to results from studies of perturbed Kerr spacetimes. Typically these studies are based on the fundamental quasinormal mode of the dominant $\ell = m = 2$ harmonic. By modeling the ringdown of accurate numerical relativity simulations, we find, in agreement with previous findings, that the fundamental mode alone is insufficient to recover the true underlying mass and spin, unless the analysis is started very late in the ringdown. Including higher overtones associated with this $\ell = m = 2$ harmonic resolves this issue, and provides an unbiased estimate of the true remnant parameters. Further, including overtones allows for the modeling of the ringdown signal for all times beyond the peak strain amplitude, indicating that the linear quasinormal regime starts much sooner than previously expected. This implies that the spacetime is well described as a linearly perturbed black hole with a fixed mass and spin as early as the peak. A model for the ringdown beginning at the peak strain amplitude can exploit the higher signal-to-noise ratio in detectors, reducing uncertainties in the extracted remnant quantities. These results should be taken into consideration when testing the no-hair theorem.

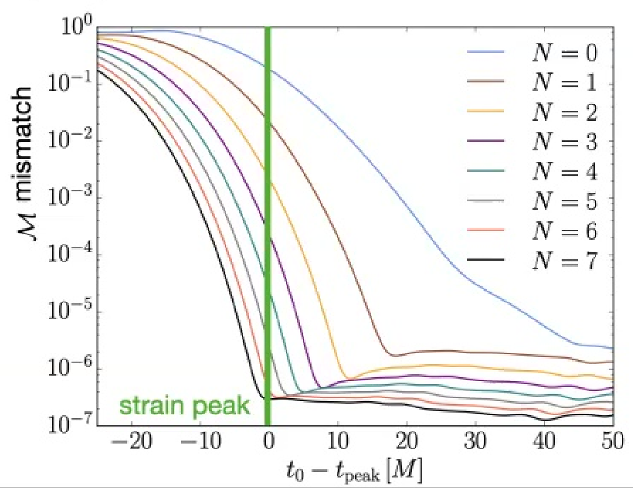

Giesler, Isi, Scheel, Teukolsky (2019)

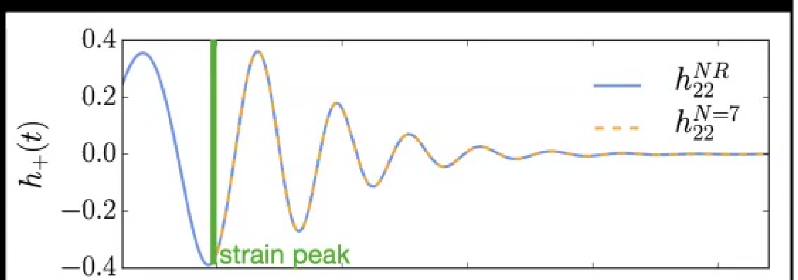

Fundamental mode ⟷ Higher overtones

N	A_0	A_1	A_2	A_3	A_4	A_5	A_6	A_7	$t_{\rm fit} - t_{\rm peak}$
0	0.971	-	-	-	-	-	-	-	47.00
1	0.974	3.89	-	-	-	-	-	-	18.48
2	0.973	4.14	8.1	-	-	-	-	-	11.85
3	0.972	4.19	9.9	11.4	-	-	-	-	8.05
4	0.972	4.20	10.6	16.6	11.6	-	-	-	5.04
5	0.972	4.21	11.0	19.8	21.4	10.1	-	-	3.01
6	0.971	4.22	11.2	21.8	28	21	6.6	-	1.50
7	0.971	4.22	11.3	23.0	33	29	14	2.9	0.00

Why are the 4th and 5th overtones dominant??
(Supported only by the fitting analysis)

1	0.974	3.89	-	-	-	-	-	-	18.48
2	0.973	4.14	8.1	-	-	-	-	-	11.85
3	0.972	4.19	9.9	11.4	-	-	-	-	8.05
4	0.972	4.20	10.6	16.6	11.6	-	-	-	5.04
7	0.971	4.22	11.3	23.0	33	29	14	2.9	0.00

Is there any theoretical reason or evidence??

Giesler, Isi, Scheel, Teukolsky (2019)

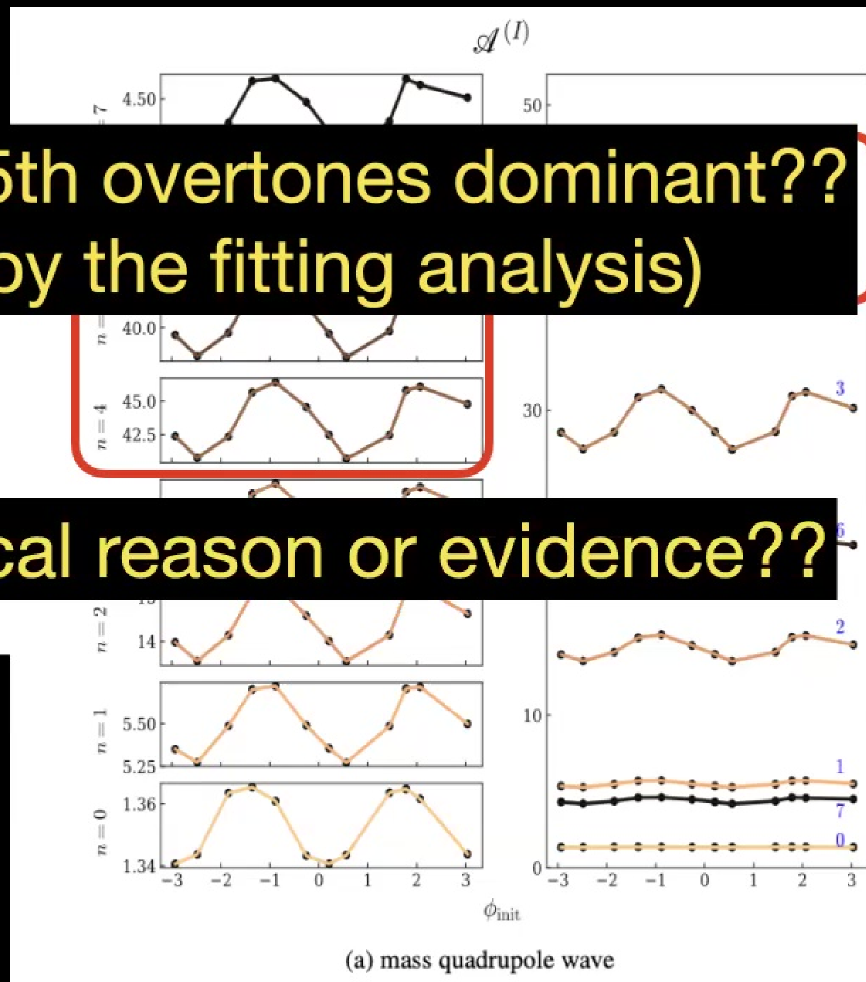

(a) mass quadrupole wave

Ma, Giesler, Varma, Scheel, and Chen (2021)

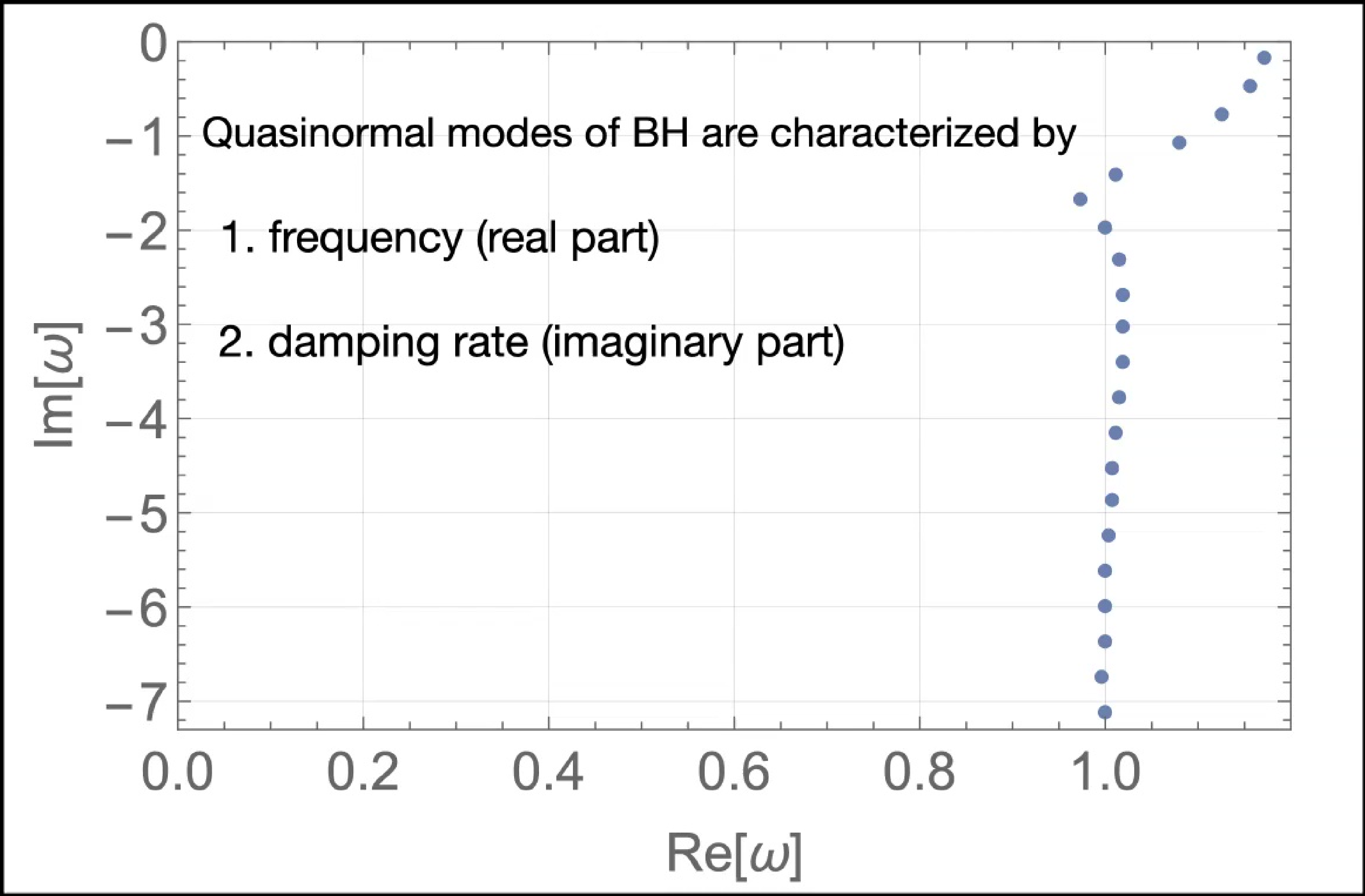
Quasinormal modes of BH are characterized by
1. frequency (real part)
2. damping rate (imaginary part)
0
−1
−2
−3
−4
−5
−6
−7
Im[ω]
0.0
0.2
0.4
0.6
0.8
1.0
Re[ω]

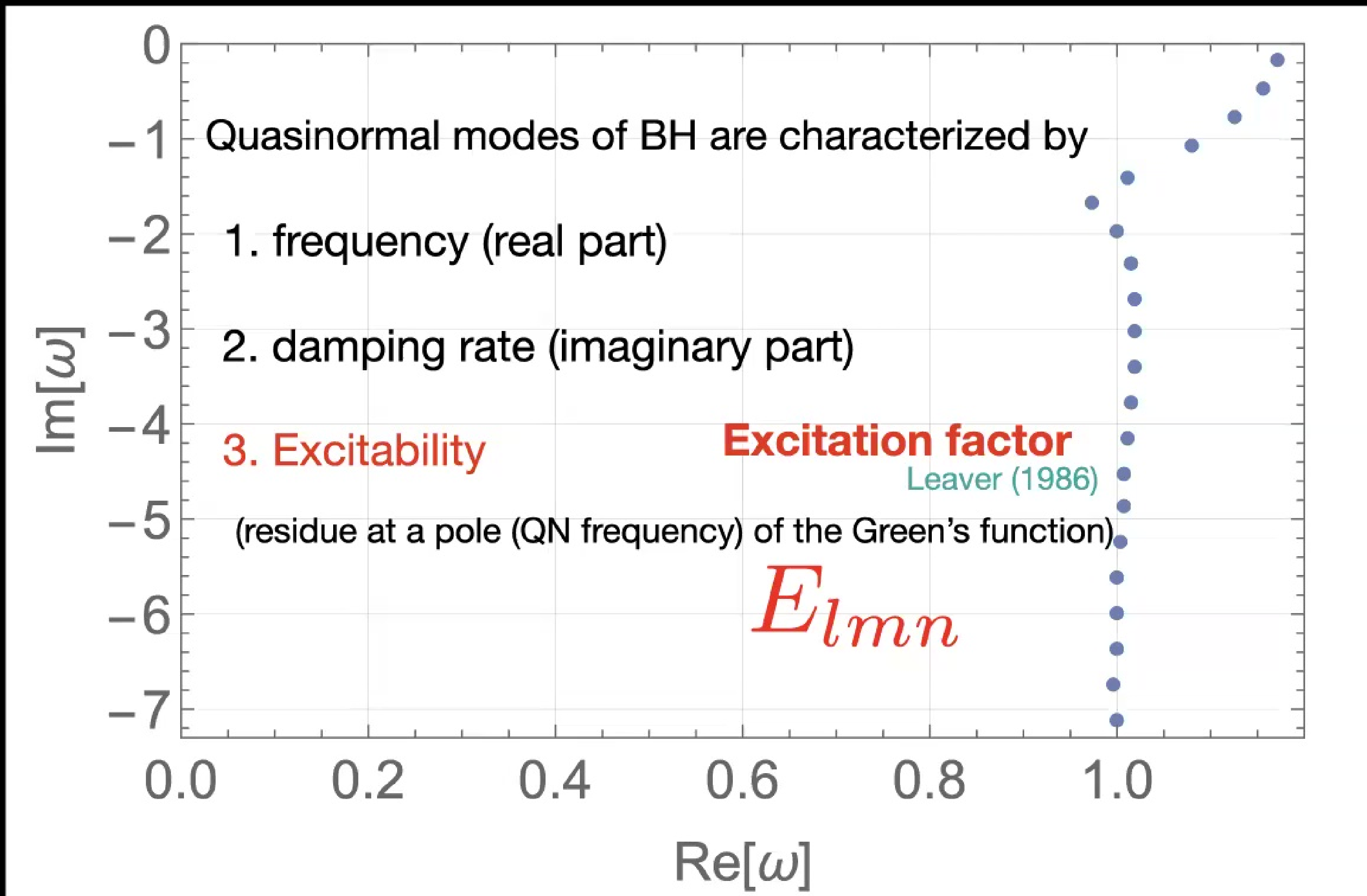
Quasinormal modes of BH are characterized by
1. frequency (real part)
2. damping rate (imaginary part)
3. Excitability
Excitation factor
Leaver (1986)
(residue at a pole (QN frequency) of the Green's function)
E_{lmn}
Im[ω]
0
−1
−2
−3
−4
−5
−6
−7
0.0
0.2
0.4
0.6
0.8
1.0
Re[ω]

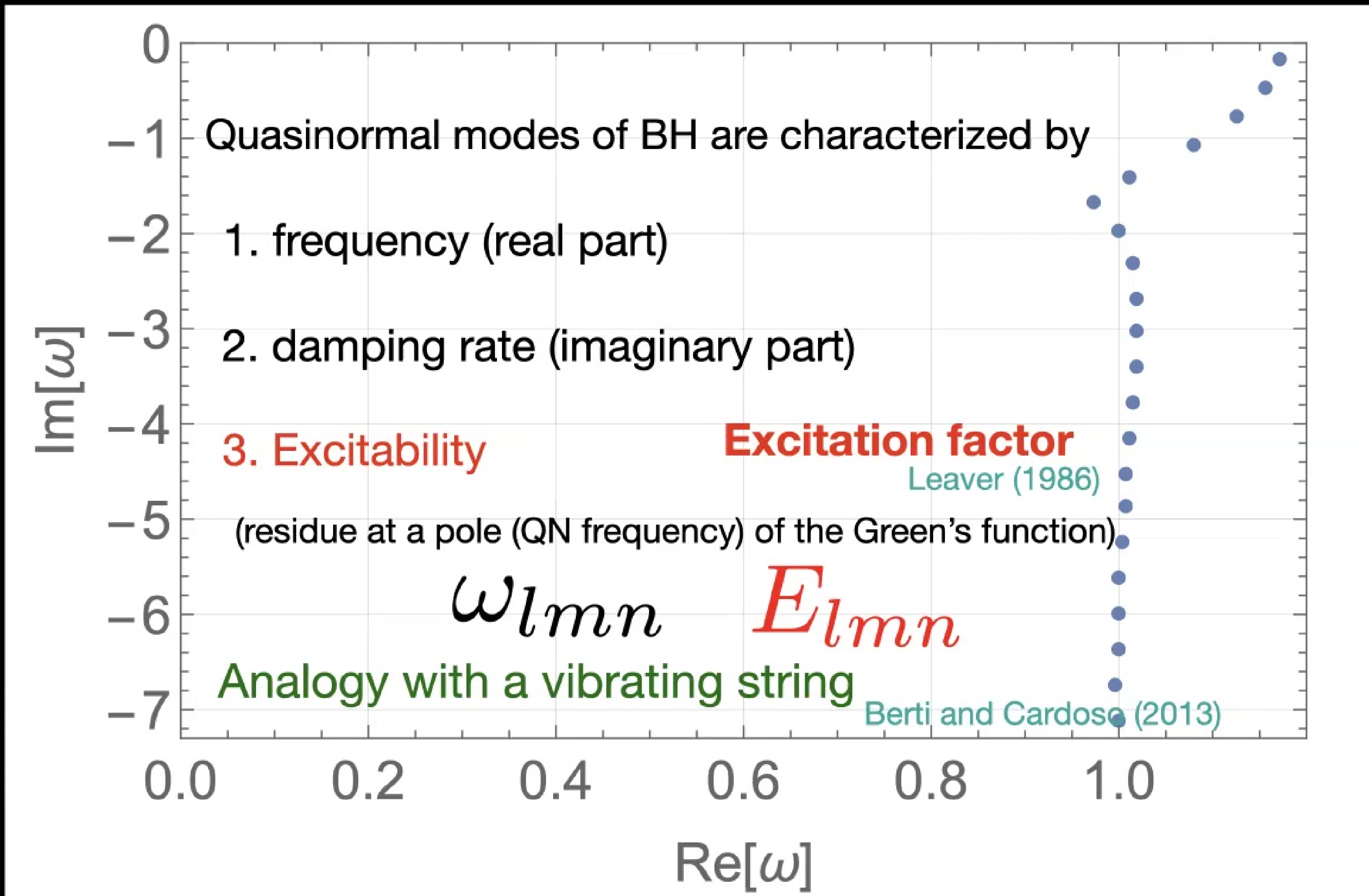
Quasinormal modes of BH are characterized by
1. frequency (real part)
2. damping rate (imaginary part)
3. Excitability
Excitation factor
Leaver (1986)
(residue at a pole (QN frequency) of the Green's function)
ω_{lmn} E_{lmn}
Analogy with a vibrating string
Berti and Cardoso (2013)
0
−1
−2
−3
−4
−5
−6
−7
Im[ω]
0.0
0.2
0.4
0.6
0.8
1.0
Re[ω]

Vibrating string

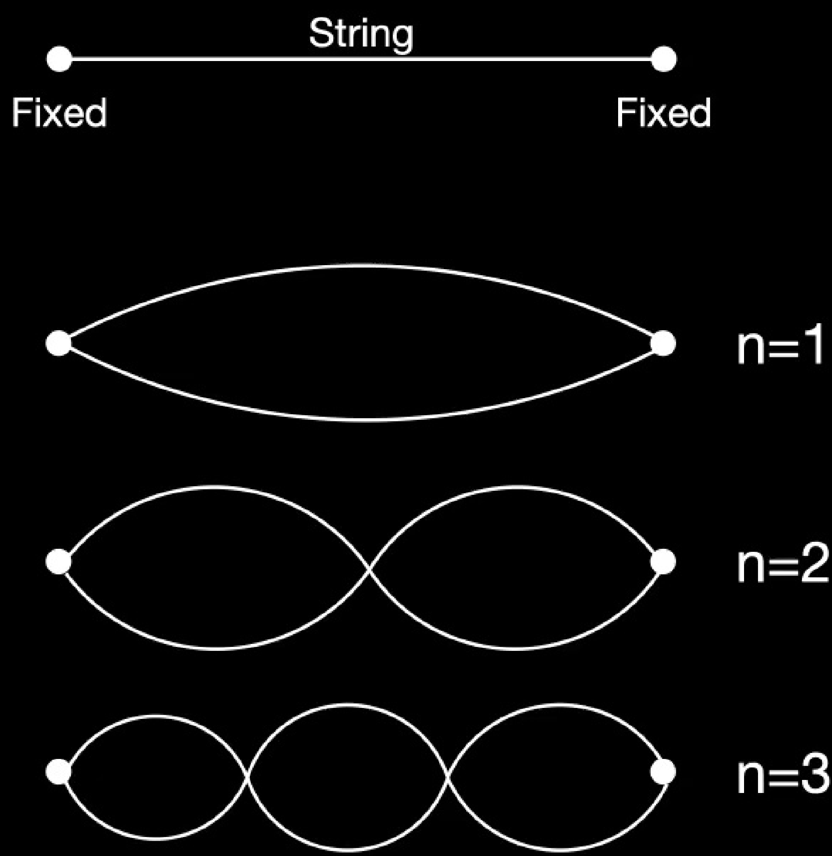

Which pattern is dominant?

Vibrating string

$$(\partial_t^2 - \partial_x^2)u(t,x) = 0 \qquad u(t,x) = \frac{1}{2\pi}\int d\omega dx' G^{(\text{string})}(x,x')\tilde{T}(\omega,x')$$

waveform — Green's function — source term

$$G(x,x') \equiv \frac{\sin\omega x' \sin\omega(x-\pi)}{\omega\sin\omega\pi} \qquad \tilde{T}(\omega,x') \equiv e^{i\omega t_0}\left(i\omega u - \frac{\partial u}{\partial t}\right)_{t=t_0}$$

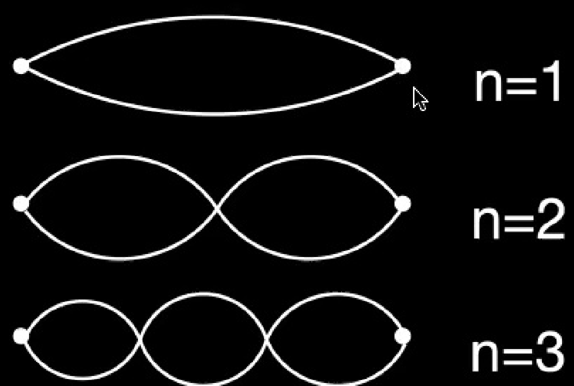

Vibrating string

$$(\partial_t^2 - \partial_x^2)u(t,x) = 0 \qquad \underbrace{u(t,x)}_{\text{waveform}} = \frac{1}{2\pi}\int d\omega dx' \underbrace{G^{(\text{string})}(x,x')}_{\text{Green's function}} \underbrace{\tilde{T}(\omega,x')}_{\text{source term}}$$

$$G(x,x') \equiv \frac{\sin\omega x' \sin\omega(x-\pi)}{\omega\sin\omega\pi} \qquad \omega\sin\omega\pi \equiv W(\omega) \qquad \tilde{T}(\omega,x') \equiv e^{i\omega t_0}\left(i\omega u - \frac{\partial u}{\partial t}\right)_{t=t_0}$$

$$= \sum_n \underbrace{E_n}_{\text{excitation factor}} \underbrace{T_n}_{\text{source factor}} \sin nx e^{-int}$$

$$E_n \equiv \frac{i}{\partial_\omega W|_{\omega=n}} = (-1)^n \frac{i}{\pi n} \propto \frac{1}{n}$$

$$T_n \equiv (-1)^n \int dx' (inu(t_0,x') - \partial_t u(t_0,x')) \sin nx'$$

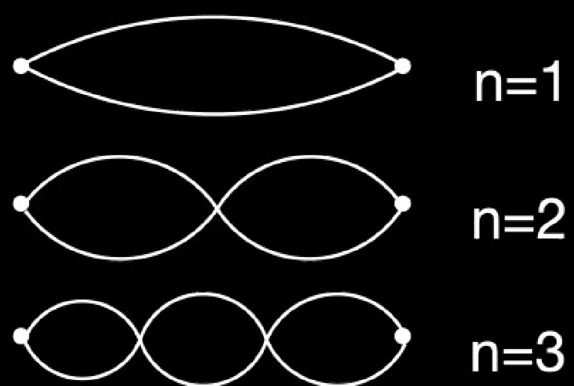

Excitation of QNMs

$$h = \frac{e^{im\phi}}{r} \int d\omega dr' \sum_{lm} e^{i\omega(r^* - t + t_0)} {}_{-2}S_{lm}(\omega, \theta) G^{(\mathrm{BH})}_{lm}(r, r') \tilde{T}_{lm}(r', \omega)$$

(spin-weighted) spheroidal harmonic function — **Green's function** — **source term**

$$= \frac{1}{r} \sum_{lmn} E_{lmn} T_{lmn} S_{lmn} e^{-i\omega_{lmn}(t - r^*)} \qquad S_{lmn} \equiv {}_{-2}S_{lm}(\omega_{lmn}, \theta)$$

Source factor:
Initial data of a distorted BH

Excitation factor:
Intrinsic quantity of BHs
Quantify the "ease-of-excitaton" of QNMs
Residues of Green's function

$$E_{lmn} \equiv \frac{A^{(\mathrm{out})}_{lm}(\omega_{lmn})}{2i\omega^3_{lmn}} \left(\frac{dA^{(\mathrm{in})}_{lm}}{d\omega} \right)^{-1}_{\omega = \omega_{lmn}}$$

Excitation of QNMs

$$h = \frac{e^{im\phi}}{r} \int d\omega dr' \sum_{lm} e^{i\omega(r^* - t + t_0)} {}_{-2}S_{lm}(\omega, \theta) G^{(\mathrm{BH})}_{lm}(r, r') \tilde{T}_{lm}(r', \omega)$$

(spin-weighted) spheroidal harmonic function — **Green's function** — **source term**

$$= \frac{1}{r} \sum_{lmn} E_{lmn} T_{lmn} S_{lmn} e^{-i\omega_{lmn}(t - r^*)} \qquad S_{lmn} \equiv {}_{-2}S_{lm}(\omega_{lmn}, \theta)$$

Source factor:
Initial data of a distorted BH

Excitation factor:
Intrinsic quantity of BHs
Quantify the "ease-of-excitaton" of QNMs
Residues of Green's function

$$E_{lmn} \equiv \frac{A^{(\mathrm{out})}_{lm}(\omega_{lmn})}{2i\omega^3_{lmn}} \left(\frac{dA^{(\mathrm{in})}_{lm}}{d\omega} \right)^{-1}_{\omega = \omega_{lmn}}$$

$$R^{(\mathrm{H})}_{lm}(\omega, r) = \begin{cases} A^{(\mathrm{trans})}_{lm}(\omega)\Delta^2 e^{-ikr^*} & \text{for } r^* \to -\infty, \\ r^{-1} A^{(\mathrm{in})}_{lm}(\omega) e^{-i\omega r^*} + r^3 A^{(\mathrm{out})}_{lm}(\omega) e^{i\omega r^*} & \text{for } r^* \to +\infty, \end{cases}$$

$$R^{(\infty)}_{lm}(\omega, r) = \begin{cases} B^{(\mathrm{in})}_{lm}(\omega)\Delta^2 e^{-ikr^*} + B^{(\mathrm{out})}_{lm}(\omega) e^{+ikr^*} & \text{for } r^* \to -\infty, \\ r^3 B^{(\mathrm{trans})}_{lm}(\omega) e^{i\omega r^*} & \text{for } r^* \to +\infty. \end{cases}$$

Excitation factor independent of the source of perturbation (universal quantity!!)

$$h_{22} = \frac{1}{r} \sum_n E_{22n} T_{22n} e^{-i\omega_{22n}(t-r^*)}$$

N.O. arXiv: 2109.09757

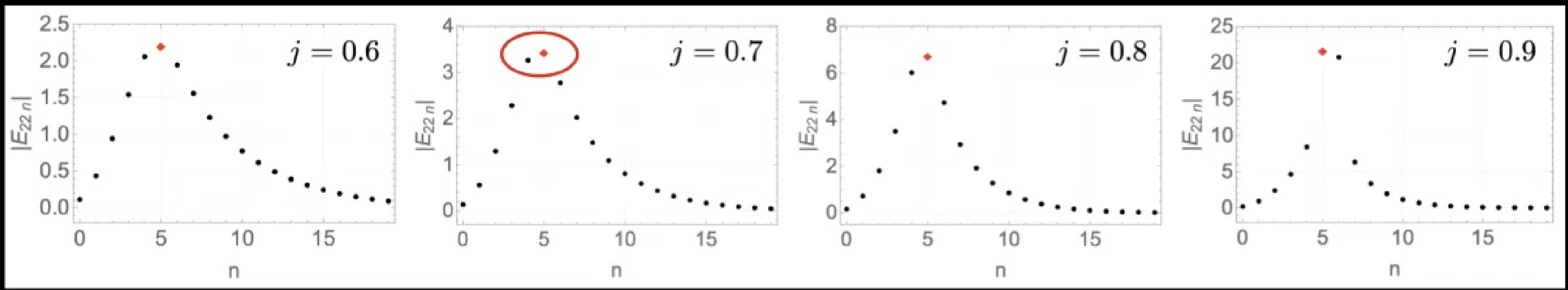

4th and 5th overtones are important!!!

N	A_0	A_1	A_2	A_3	A_4	A_5	A_6	A_7	$t_{\rm fit} - t_{\rm peak}$
0	0.971	-	-	-	-	-	-	-	47.00
1	0.974	3.89	-	-	-	-	-	-	18.48
2	0.973	4.14	8.1	-	-	-	-	-	11.85
3	0.972	4.19	9.9	11.4	-	-	-	-	8.05
4	0.972	4.20	10.6	16.6	11.6	-	-	-	5.04
5	0.972	4.21	11.0	19.8	21.4	10.1	-	-	3.01
6	0.971	4.22	11.2	21.8	28	21	6.6	-	1.50
7	0.971	4.22	11.3	23.0	33	29	14	2.9	0.00

Giesler, Isi, Scheel, Teukolsky (2019)

Excitation factor independent of the source of perturbation (universal quantity!!)

$$h_{22} = \frac{1}{r} \sum_n E_{22n} T_{22n} e^{-i\omega_{22n}(t-r^*)}$$

N.O. arXiv: 2109.09757

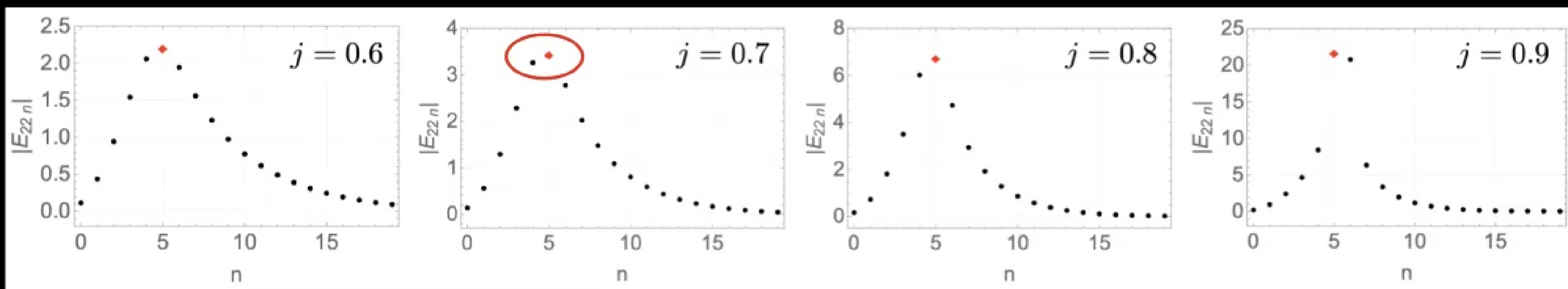

If the source factors have strong dependence on the overtone number “n”, the behaviour of the excitation factor is NOT meaningful…

4	0.972	4.20	10.6	16.6	11.6	-	-	-	5.04
5	0.972	4.21	11.0	19.8	21.4	10.1	-	-	3.01
6	0.971	4.22	11.2	21.8	28	21	6.6	-	1.50
7	0.971	4.22	11.3	23.0	33	29	14	2.9	0.00

Giesler, Isi, Scheel, Teukolsky (2019)

$$h_{22} = \frac{1}{r} \sum_n C_{22n} \, {}_{-2}S_{22n} e^{-i\omega_{22n}(t-r^*)}$$

challenging to compute!

$$C_{22n} = E_{22n} T_{22n}$$

excitation coefficients

excitation factor

source factor

Giesler, Isi, Scheel, Teukolsky (2019)

N	A_0	A_1	A_2	A_3	A_4	A_5	A_6	A_7	$t_{\rm fit} - t_{\rm peak}$
0	0.971	-	-	-	-	-	-	-	47.00
1	0.974	3.89	-	-	-	-	-	-	18.48
2	0.973	4.14	8.1	-	-	-	-	-	11.85
3	0.972	4.19	9.9	11.4	-	-	-	-	8.05
4	0.972	4.20	10.6	16.6	11.6	-	-	-	5.04
5	0.972	4.21	11.0	19.8	21.4	10.1	-	-	3.01
6	0.971	4.22	11.2	21.8	28	21	6.6	-	1.50
7	0.971	4.22	11.3	23.0	33	29	14	2.9	0.00

$$h_{22} = \frac{1}{r} \sum_n C_{22n\ -2}S_{22n} e^{-i\omega_{22n}(t-r^*)}$$

challenging to compute!

$$C_{22n} = E_{22n} T_{22n}$$

excitation coefficients

excitation factor

source factor

Giesler, Isi, Scheel, Teukolsky (2019)

N	A_0	A_1	A_2	A_3	A_4	A_5	A_6	A_7	$t_{\rm fit} - t_{\rm peak}$
0	0.971	-	-	-	-	-	-	-	47.00
1	0.974	3.89	-	-	-	-	-	-	18.48
2	0.973	4.14	8.1	-	-	-	-	-	11.85
3	0.972	4.19	9.9	11.4	-	-	-	-	8.05
4	0.972	4.20	10.6	16.6	11.6	-	-	-	5.04
5	0.972	4.21	11.0	19.8	21.4	10.1	-	-	3.01
6	0.971	4.22	11.2	21.8	28	21	6.6	-	1.50
7	0.971	4.22	11.3	23.0	33	29	14	2.9	0.00

N.O. (2021)

overtone number	$j = 0.7$		$j = 0.8$		$j = 0.9$		$j = 0.99$	
n	$\|E_{22n}\|$	$\arg(E_{22n})$	$\|E_{22n}\|$	$\arg(E_{22n})$	$\|E_{22n}\|$	$\arg(E_{22n})$	$\|E_{22n}\|$	$\arg(E_{22n})$
0	0.136	0.879	0.164	1.17	0.194	1.62	0.148	2.71
1	0.557	−1.31	0.725	−0.917	0.927	−0.292	0.716	1.15
2	1.29	2.64	1.80	−3.10	2.39	−2.22	1.81	−0.285
3	2.28	0.155	3.50	0.885	4.63	2.12	3.25	−1.62
4	3.26	−2.56	6.01	−1.68	8.40	0.250	4.68	−2.88
5	3.44	0.825	6.75	1.70	21.6	2.60	0.505	0.747
6	2.77	−2.04	4.72	−1.13	20.8	−0.605	5.76	2.22
7	2.02	1.49	2.93	2.62	6.31	−2.01	6.30	1.10
8	1.48	−1.20	1.92	0.170	3.36	2.34	6.28	0.0509
9	1.09	2.40	1.28	−2.26	1.96	0.362	5.80	−0.94
10	0.802	−0.278	0.860	1.58	1.17	−1.63	5.03	−1.87
11	0.591	−2.96	0.576	−0.852	0.701	2.66	4.11	−2.76
12	0.435	0.640	0.384	2.99	0.419	0.657	3.18	2.68
13	0.318	−2.04	0.254	0.550	0.249	−1.34	2.33	1.87
14	0.231	1.54	0.167	−1.89	0.147	2.94	1.62	1.06
15	0.168	−1.14	0.109	1.94	0.0869	0.936	1.09	0.268
16	0.121	2.44	0.0714	−0.500	0.0508	−1.06	0.710	−0.534
17	0.0873	−0.249	0.0461	−2.95	0.0295	−3.07	0.453	−1.34
18	0.0624	−2.94	0.0296	0.883	0.0171	1.21	0.285	−2.16
19	0.0443	0.635	0.0189	−1.57	0.00983	−0.792	0.178	−2.98
20	0.0313	−2.07	0.0120	2.24	0.00563	−2.80	0.110	2.48

$$h_{22} = \frac{1}{r} \sum_n C_{22n\, -2}S_{22n} e^{-i\omega_{22n}(t-r^*)}$$

~~challenging to compute!~~

easy to estimate!!

$$C_{22n} = E_{22n} T_{22n}$$

excitation coefficients — excitation factor — source factor

Giesler, Isi, Scheel, Teukolsky (2019)

N	A_0	A_1	A_2	A_3	A_4	A_5	A_6	A_7	$t_{\rm fit} - t_{\rm peak}$
0	0.971	-	-	-	-	-	-	-	47.00
1	0.974	3.89	-	-	-	-	-	-	18.48
2	0.973	4.14	8.1	-	-	-	-	-	11.85
3	0.972	4.19	9.9	11.4	-	-	-	-	8.05
4	0.972	4.20	10.6	16.6	11.6	-	-	-	5.04
5	0.972	4.2							
6	0.971	4.2							
7	0.971	4.2							

N.O. (2021)

overtone number	$j = 0.7$		$j = 0.8$		$j = 0.9$		$j = 0.99$	
n	$\lvert E_{22n}\rvert$	$\arg(E_{22n})$	$\lvert E_{22n}\rvert$	$\arg(E_{22n})$	$\lvert E_{22n}\rvert$	$\arg(E_{22n})$	$\lvert E_{22n}\rvert$	$\arg(E_{22n})$
0	0.136	0.879	0.164	1.17	0.194	1.62	0.148	2.71
1	0.557	−1.31	0.725	−0.917	0.927	−0.292	0.716	1.15
2	1.29	2.64	1.80	−3.10	2.39	−2.22	1.81	−0.285
3	2.28	0.155	3.50	0.885	4.63	2.12	3.25	−1.62
4	3.26	−2.56	6.01	−1.68	8.40	0.250	4.68	−2.88
5	3.44	0.825	6.75	1.70	21.6	2.60	0.505	0.747
6	2.77	−2.04	4.72	−1.13	20.8	−0.605	5.76	2.22
								1.10
								0.0509
								−0.94
								−1.87
								−2.76
								2.68
								1.87
								1.06
								0.268
								−0.534
								−1.34
								−2.16
								−2.98
								2.48

n	0	1	2	3	4	5	6	7
$\lvert E_{22n}\rvert$	0.135	0.546	1.26	2.21	3.13	3.31	2.69	1.98
$\lvert T_{22n}\rvert$	7.21	7.72	8.96	10.4	10.5	8.76	5.21	1.47
$\lvert E_{22n}\rvert / \lvert E_{220}\rvert$	1	4.06	9.37	16.4	23.3	24.6	20.0	14.7
$\lvert T_{22n}\rvert / \lvert T_{220}\rvert$	1	1.07	1.24	1.44	1.46	1.21	0.72	0.203

$$h_{22} = \frac{1}{r} \sum_n C_{22n} \, {}_{-2}S_{22n} e^{-i\omega_{22n}(t-r^*)}$$

~~challenging to compute!~~

easy to estimate!!

$$C_{22n} = E_{22n} T_{22n}$$

excitation coefficients | excitation factor | source factor

Giesler, Isi, Scheel, Teukolsky (2019)

N	A_0	A_1	A_2	A_3	A_4	A_5	A_6	A_7	$t_{\rm fit} - t_{\rm peak}$
0	0.971	-	-	-	-	-	-	-	47.00
1	0.974	3.89	-	-	-	-	-	-	18.48
2	0.973	4.14	8.1	-	-	-	-	-	11.85
3	0.972	4.19	9.9	11.4	-	-	-	-	8.05
4	0.972	4.20	10.6	16.6	11.6	-	-	-	5.04
5	0.972	4.2							
6	0.971	4.2							
7	0.971	4.2							

N.O. (2021)

overtone number	$j = 0.7$		$j = 0.8$		$j = 0.9$		$j = 0.99$	
n	$\lvert E_{22n} \rvert$	$\arg(E_{22n})$	$\lvert E_{22n} \rvert$	$\arg(E_{22n})$	$\lvert E_{22n} \rvert$	$\arg(E_{22n})$	$\lvert E_{22n} \rvert$	$\arg(E_{22n})$
0	0.136	0.879	0.164	1.17	0.194	1.62	0.148	2.71
1	0.557	−1.31	0.725	−0.917	0.927	−0.292	0.716	1.15
2	1.29	2.64	1.80	−3.10	2.39	−2.22	1.81	−0.285
3	2.28	0.155	3.50	0.885	4.63	2.12	3.25	−1.62
4	3.26	−2.56	6.01	−1.68	8.40	0.250	4.68	−2.88
5	3.44	0.825	6.75	1.70	21.6	2.60	0.505	0.747
6	2.77	−2.04	4.72	−1.13	20.8	−0.605	5.76	2.22
								1.10
								0.0509
								−0.94
								−1.87
								−2.76
								2.68
								1.87
								1.06
								0.268
								−0.534
								−1.34
								−2.16
								−2.98
								2.48

n	0	1	2	3	4	5	6	7
$\lvert E_{22n} \rvert$	0.135	0.546	1.26	2.21	3.13	3.31	2.69	1.98
$\lvert T_{22n} \rvert$	7.21	7.72	8.96	10.4	10.5	8.76	5.21	1.47
$\lvert E_{22n} \rvert / \lvert E_{220} \rvert$	1	4.06	9.37	16.4	23.3	24.6	20.0	14.7
$\lvert T_{22n} \rvert / \lvert T_{220} \rvert$	1	1.07	1.24	1.44	1.46	1.21	0.72	0.203

Excitation factor is SENSITIVE to "n"

Source factor is INSENSITIVE to "n"

$$h_{22} = \frac{1}{r} \sum_n C_{22n\,-2}S_{22n}\, e^{-i\omega_{22n}(t-r^*)}$$

~~challenging to compute!~~

easy to estimate!!

$$C_{22n} = E_{22n} T_{22n}$$

excitation coefficients — excitation factor — source factor

Giesler, Isi, Scheel, Teukolsky (2019)

N	A_0	A_1	A_2	A_3	A_4	A_5	A_6	A_7	$t_{\rm fit} - t_{\rm peak}$
0	0.971	-	-	-	-	-	-	-	47.00
1	0.974	3.89	-	-	-	-	-	-	18.48
2	0.973	4.14	8.1	-	-	-	-	-	11.85
3	0.972	4.19	9.9	11.4	-	-	-	-	8.05
4	0.972	4.20	10.6	16.6	11.6	-	-	-	5.04
5	0.972	4.2							
6	0.971	4.2							
7	0.971	4.2							

N.O. (2021)

overtone number	$j = 0.7$		$j = 0.8$		$j = 0.9$		$j = 0.99$	
n	$\lvert E_{22n}\rvert$	$\arg(E_{22n})$	$\lvert E_{22n}\rvert$	$\arg(E_{22n})$	$\lvert E_{22n}\rvert$	$\arg(E_{22n})$	$\lvert E_{22n}\rvert$	$\arg(E_{22n})$
0	0.136	0.879	0.164	1.17	0.194	1.62	0.148	2.71
1	0.557	−1.31	0.725	−0.917	0.927	−0.292	0.716	1.15
2	1.29	2.64	1.80	−3.10	2.39	−2.22	1.81	−0.285
3	2.28	0.155	3.50	0.885	4.63	2.12	3.25	−1.62
4	3.26	−2.56	6.01	−1.68	8.40	0.250	4.68	−2.88
5	3.44	0.825	6.75	1.70	21.6	2.60	0.505	0.747
6	2.77	−2.04	4.72	−1.13	20.8	−0.605	5.76	2.22
								1.10
								0.0509
								−0.94
								−1.87
								−2.76
								2.68
								1.87
								1.06
								0.268
								−0.534
								−1.34
								−2.16
								−2.98
								2.48

n	0	1	2	3	4	5	6	7
$\lvert E_{22n}\rvert$	0.135	0.546	1.26	2.21	3.13	3.31	2.69	1.98
$\lvert T_{22n}\rvert$	7.21	7.72	8.96	10.4	10.5	8.76	5.21	1.47
$\lvert E_{22n}\rvert / \lvert E_{220}\rvert$	1	4.06	9.37	16.4	23.3	24.6	20.0	14.7
$\lvert T_{22n}\rvert / \lvert T_{220}\rvert$	1	1.07	1.24	1.44	1.46	1.21	0.72	0.203

Excitation factor is SENSITIVE to "n"

Source factor is INSENSITIVE to "n" (equipartition??)

Binary Black Hole with the comparable mass ratio

Black hole ringdown: the importance of overtones

Matthew Giesler,[1,*] Maximiliano Isi,[2,3,†] Mark A. Scheel,[1] and Saul A. Teukolsky[1,4]
[1]Walter Burke Institute for Theoretical Physics, California Institute of Technology, Pasadena, CA 91125, USA
[2]LIGO Laboratory, Massachusetts Institute of Technology, Cambridge, Massachusetts 02139, USA
[3]LIGO Laboratory, California Institute of Technology, Pasadena, California 91125, USA
[4]Cornell Center for Astrophysics and Planetary Science, Cornell University, Ithaca, New York 14853,
(Dated: January 13, 2020)

It is possible to infer the mass and spin of the remnant black hole from binary black hole mergers by comparing the ringdown gravitational wave signal to results from studies of perturbed Kerr spacetimes. Typically these studies are based on the fundamental quasinormal mode of the dominant $\ell = m = 2$ harmonic. By modeling the ringdown of accurate numerical relativity simulations, we find, in agreement with previous findings, that the fundamental mode alone is insufficient to recover the true underlying mass and spin, unless the analysis is started very late in the ringdown. Including higher overtones associated with this $\ell = m = 2$ harmonic resolves this issue, and provides an unbiased estimate of the true remnant parameters. Further, including overtones allows for the modeling of the ringdown signal for all times beyond the peak strain amplitude, indicating that the linear quasinormal regime starts much sooner than previously expected. This implies that the spacetime is well described as a linearly perturbed black hole with a fixed mass and spin as early as the peak. A model for the ringdown beginning at the peak strain amplitude can exploit the higher signal-to-noise ratio in detectors, reducing uncertainties in the extracted remnant quantities. These results should be taken into consideration when testing the no-hair theorem.

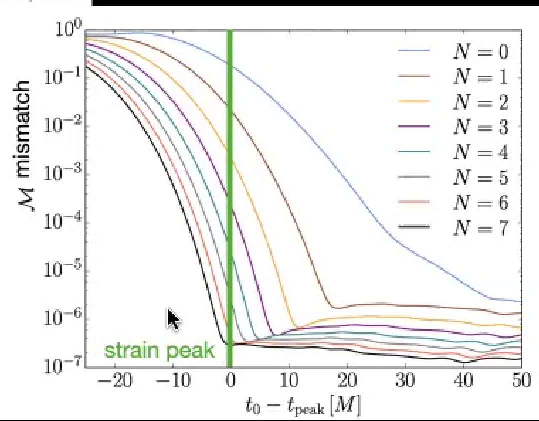

Giesler, Isi, Scheel, Teukolsky (2019)

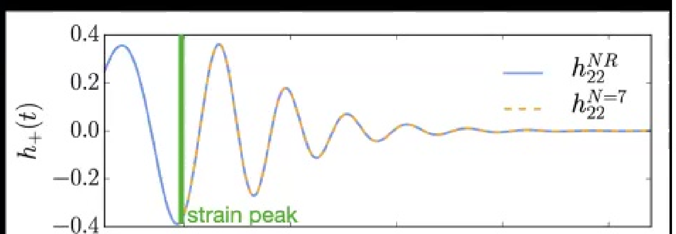

Fundamental mode ⟷ Higher overtones

N	A_0	A_1	A_2	A_3	A_4	A_5	A_6	A_7	$t_{\rm fit} - t_{\rm peak}$
0	0.971	-	-	-	-	-	-	-	47.00
1	0.974	3.89	-	-	-	-	-	-	18.48
2	0.973	4.14	8.1	-	-	-	-	-	11.85
3	0.972	4.19	9.9	11.4	-	-	-	-	8.05
4	0.972	4.20	10.6	16.6	11.6	-	-	-	5.04
5	0.972	4.21	11.0	19.8	21.4	10.1	-	-	3.01
6	0.971	4.22	11.2	21.8	28	21	6.6	-	1.50
7	0.971	4.22	11.3	23.0	33	29	14	2.9	0.00

$$h_{22} = \frac{1}{r} \sum_{n} C_{22n\,-2}S_{22n}\, e^{-i\omega_{22n}(t-r^*)}$$

~~challenging to compute!~~

easy to estimate!!

$C \quad = E \quad T$

"Importance of overtones" is determined mostly by the excitation factors!!

The equipartition theorem might hold in BH ringing after a merger event.

n	0	1	2	3	4	5	6	7
$\|E_{22n}\|$	0.135	0.546	1.26	2.21	3.13	3.31	2.69	1.98
$\|T_{22n}\|$	7.21	7.72	8.96	10.4	10.5	8.76	5.21	1.47
$\|E_{22n}\|/\|E_{220}\|$	1	4.06	9.37	16.4	23.3	24.6	20.0	14.7
$\|T_{22n}\|/\|T_{220}\|$	1	1.07	1.24	1.44	1.46	1.21	0.72	0.203

−1.87
−2.76
2.68
1.87
1.06
0.268
−0.534
−1.34
−2.16
−2.98
2.48

Excitation factor is SENSITIVE to "n"

Source factor is INSENSITIVE to "n" (equipartition??)

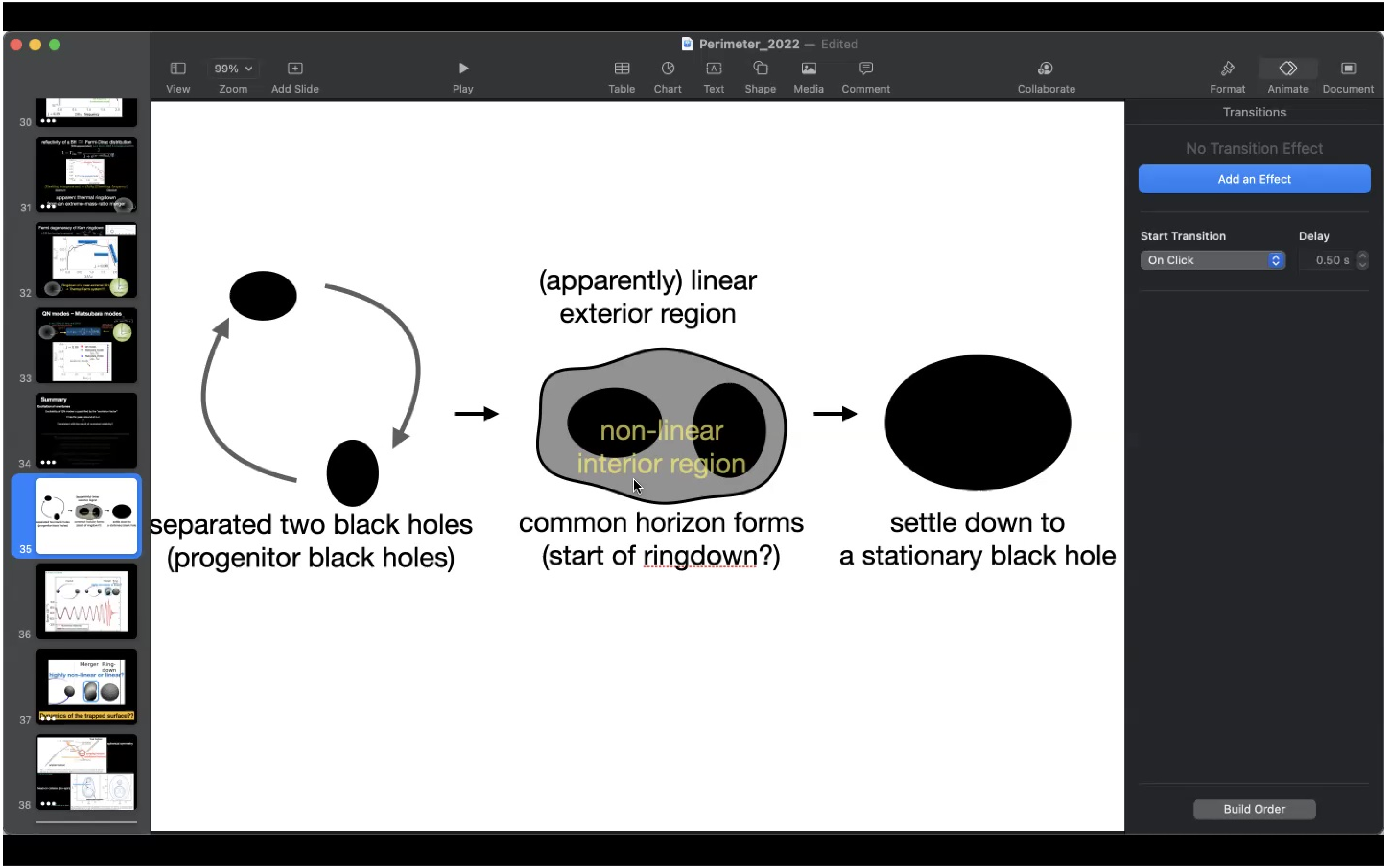
Perimeter_2022 — Edited
(apparently) linear
exterior region
non-linear
interior region
separated two black holes
(progenitor black holes)
common horizon forms
(start of ringdown?)
settle down to
a stationary black hole
Transitions
No Transition Effect
Add an Effect
Start Transition
On Click
Delay
0.50 s
Build Order

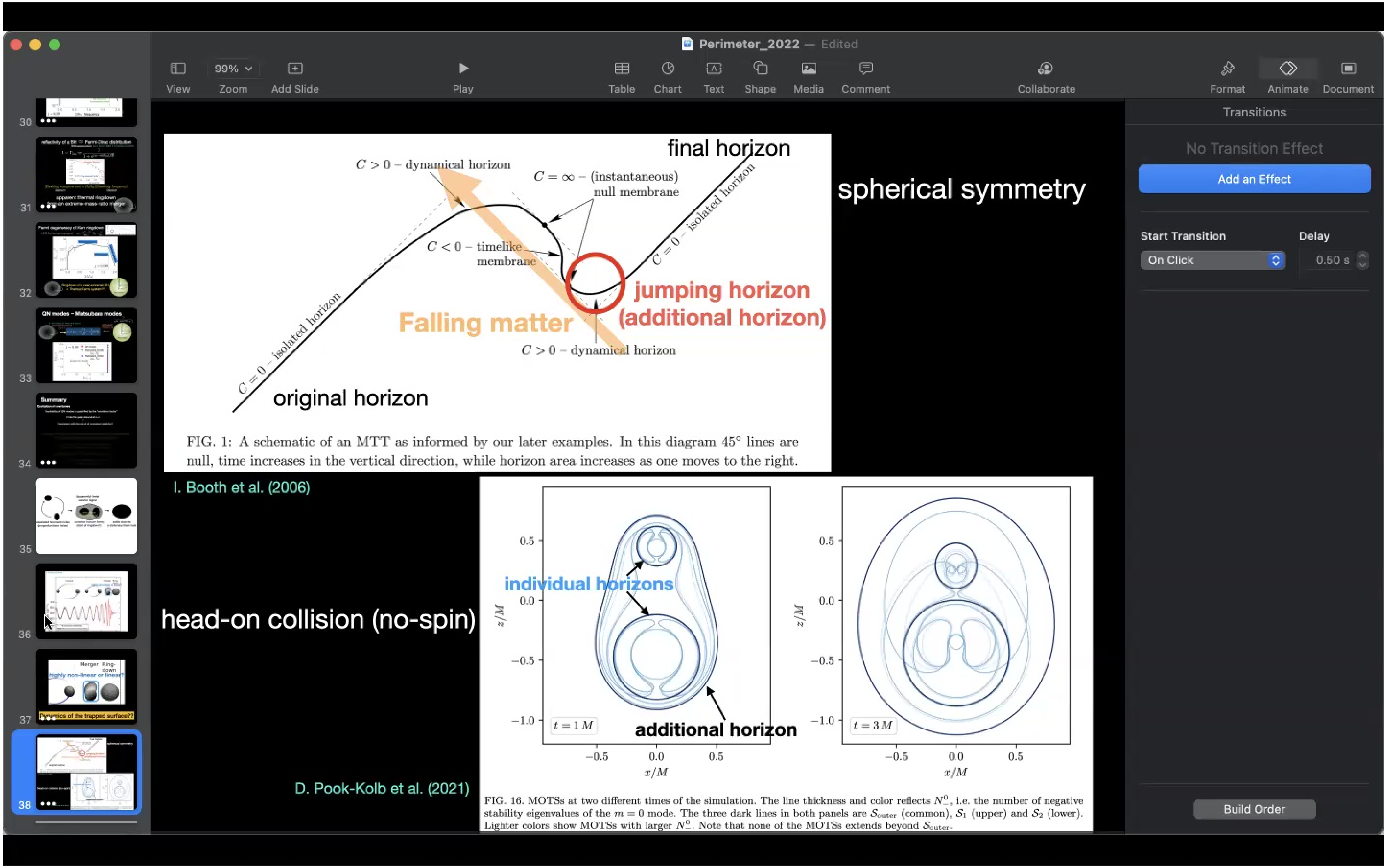
Perimeter_2022 — Edited
final horizon
$C > 0$ – dynamical horizon
$C = \infty$ – (instantaneous) null membrane
$C = 0$ – isolated horizon
spherical symmetry
$C < 0$ – timelike membrane
jumping horizon (additional horizon)
Falling matter
$C > 0$ – dynamical horizon
$C = 0$ – isolated horizon
original horizon
FIG. 1: A schematic of an MTT as informed by our later examples. In this diagram 45° lines are null, time increases in the vertical direction, while horizon area increases as one moves to the right.
I. Booth et al. (2006)
individual horizons
head-on collision (no-spin)
additional horizon
$t = 1\,M$
$t = 3\,M$
x/M
z/M
D. Pook-Kolb et al. (2021)
FIG. 16. MOTSs at two different times of the simulation. The line thickness and color reflects N_-^0, i.e. the number of negative stability eigenvalues of the $m = 0$ mode. The three dark lines in both panels are $\mathcal{S}_{\rm outer}$ (common), $\mathcal{S}_1$ (upper) and $\mathcal{S}_2$ (lower). Lighter colors show MOTSs with larger N_-^0. Note that none of the MOTSs extends beyond $\mathcal{S}_{\rm outer}$.

Difficulty in the measurement of the damping time

GW150914

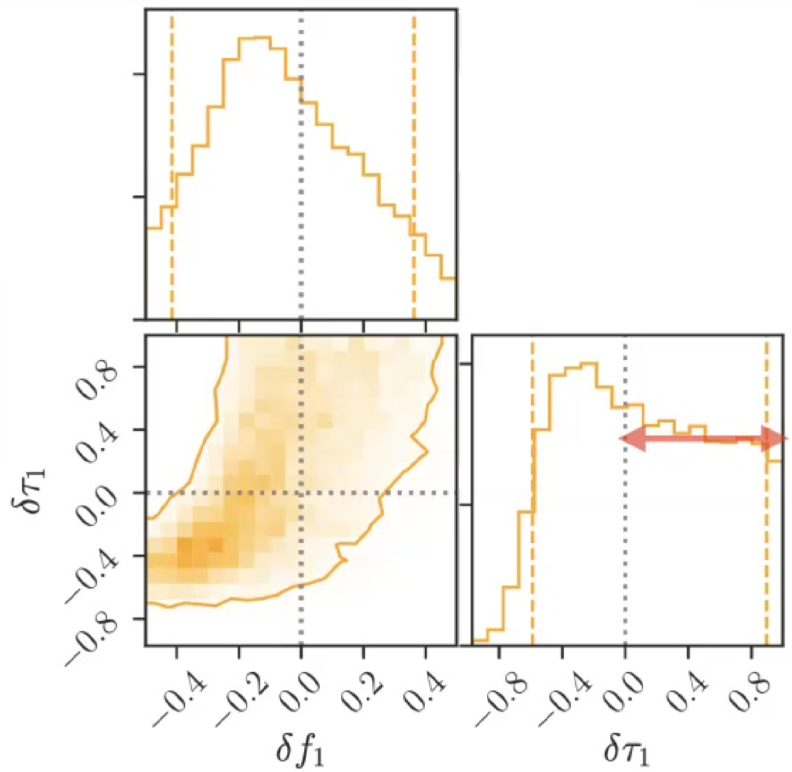

FIG. 4. Measurement of the frequency and damping time of the first overtone, using data starting at the peak. The colormap represents the posterior distribution of the fractional deviations δf_1 and $\delta\tau_1$ away from the no-hair value $\delta f_1 = \delta\tau_1 = 0$ (gray dotted lines). The solid contour and dashed vertical lines enclose 90% of the posterior probability. All other parameters, including M_f and χ_f have been marginalized away. Fixing $\delta f_1 = \delta\tau_1 = 0$ recovers the $N = 1$ analysis in Figs. 1 and 3.

M. Isi et al. (2019)

frequency of the first overtone

$$f_{221} = (1 + \delta f_1) \times f_{221}^{(\mathrm{GR})}$$

decay time of the first overtone

$$\tau_{221} = (1 + \delta\tau_1) \times \tau_{221}^{(\mathrm{GR})}$$

inferred peak of the strain. Fig. 4 shows the resulting marginalized posterior over the fractional frequency and damping time deviations (δf_1 and $\delta\tau_1$ respectively). With 68% credibility, we measure $\delta f_1 = -0.05 \pm 0.2$. To that level of credibility, this establishes agreement with the no-hair hypothesis ($\delta f_1 = 0$) at the 20% level. The damping time is largely unconstrained in the $-0.06 \lesssim \delta\tau_1 \lesssim 1$ range. This has little impact on the frequency measurement, which is unaffected by setting $\delta\tau_1 = 0$. We find that the ratio of marginal likelihoods (the Bayes factor) between the no-hair model ($\delta f_1 = \delta\tau_1 = 0$) and our floating frequency and damping time model is 1.75.

Rapidly spinning supermassive BHs

C. S. Reynolds (2021) review paper

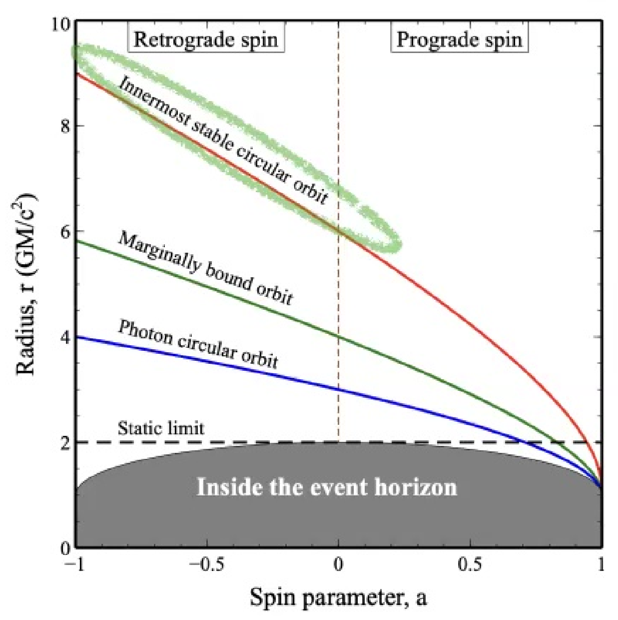

Table 1 : Summary of published AGN/SMBH spin measurements from the X-ray reflection method in approximate order of increasing mass. Reflecting the conventions in the primary literature, all masses are quoted with 1σ error bars whereas spins are quoted with 90 per cent error ranges.

Object	Mass ($\times 10^6 M_\odot$)	Spin	Mass/Spin References
Mrk359	~ 1.1	$0.66^{+0.30}_{-0.54}$	Va16+
Ark564	~ 1.1	> 0.9	Va16+/Ji19
Mrk766	$1.8^{+1.6}_{-1.4}$	> 0.92	Be06/Bu18
NGC4051	1.91 ± 0.78	> 0.99	Va16+
NGC1365	~ 2	> 0.97	Va16+/Wa14
1H0707-495	~ 2.3	> 0.94	Va16+/Ka15
MCG–6-30-15	$2.9^{+1.8}_{-1.6}$	$0.91^{+0.06}_{-0.07}$	Va16+/Ma13
NGC5506	~ 5	0.93 ± 0.04	Ni09/Su18
IRAS13224–3809	~ 6.3	> 0.975	Va16+/Ji18
Tons180	~ 8.1	> 0.98	Va16+/Ji19
ESO 362–G18	12.5 ± 4.5	> 0.92	VA16+
Swift J2127.4+5654	~ 15	$0.72^{+0.14}_{-0.20}$	Va16+/Ji19
Mrk335	$17.8^{+4.6}_{-3.7}$	> 0.99	Gr18/Ji19
Mrk110	25.1 ± 6.1	> 0.99	Va16+/Ji19
NGC3783	29.8 ± 5.4	> 0.88	Va16+
1H0323+342	34^{+9}_{-6}	> 0.9	Wa16/Gh18
NGC 4151	$45.7^{+5.7}_{-4.7}$	> 0.9	Be06/Ke15
Mrk79	52.4 ± 14.4	> 0.5	Va16+/Ji19
PG1229+204	57 ± 25	$0.93^{+0.06}_{-0.02}$	Ji19/Ji19
IRAS13197-1627	~ 64	> 0.7	Va10/Wa18
3C120	69^{+31}_{-24}	> 0.95	Gr18/Va16+
Mrk841	~ 79	> 0.52	Va16+
IRAS09149–6206	~ 100	$0.94^{+0.02}_{-0.07}$	Wa20/Wa20
Ark120	150 ± 19	> 0.85	Va16+/Ji19
RBS1124	~ 180	> 0.8	Mi10/Ji19
RXS J1131-1231	~ 200	$0.87^{+0.08}_{-0.15}$	Sl12/Re14c
Fairall 9	255 ± 56	$0.52^{+0.19}_{-0.15}$	Va16+
1H0419-577	~ 340	> 0.98	Va16+/Ji19a
PG0804+761	550 ± 60	> 0.97	Ji19/Ji19
Q2237+305	~ 1000	$0.74^{+0.06}_{-0.03}$	Ass11/Re14b
PG2112+059	~ 1000	> 0.83	Ve06/Sc10
H1821+643	4500 ± 1500	> 0.4	Va16+
IRAS 00521–7054	—	> 0.77	–/Wa19
IRAS13349+2438	—	$0.93^{+0.03}_{-0.02}$	–/Pa18
Fairall 51	—	> 0.75	–/Sv15
Mrk 1501	—	> 0.97	–/Ch19

NO and Daichi Tsuna arXiv: 2210.14049

RIKEN-iTHEMS-Report-22
RESCEU-19/22

Slowly Decaying Ringdown of a Rapidly Spinning Black Hole: Probing the No-Hair Theorem by Small Mass-Ratio Mergers with LISA

Naritaka Oshita[1*] and Daichi Tsuna[2†]
[1] *RIKEN iTHEMS, Wako, Saitama, Japan, 351-0198* and
[2] *Research Center for the Early Universe (RESCEU),*
Graduate School of Science, The University of Tokyo,
7-3-1 Hongo, Bunkyo-ku, Tokyo 113-0033, Japan

The detectability of multiple quasi-normal (QN) modes, including overtones and higher harmonics, with the Laser Interferometer Space Antenna (LISA) is investigated by computing the gravitational wave (GW) signal induced by an intermediate or extreme mass ratio merger involving a supermassive black hole (SMBH). We confirm that the ringdown of rapidly spinning black holes are long-lived, and higher harmonics of the ringdown are significantly excited for mergers of small mass ratios. We demonstrate that the observation of GWs from rapidly rotating SMBHs has a significant advantage for detecting multiple QN modes and testing the no-hair theorem of black holes with high accuracy.

Slowly decaying ringdown of a rapidly spinning Kerr BH

NO and Daichi Tsuna (2022)

Rich angular modes

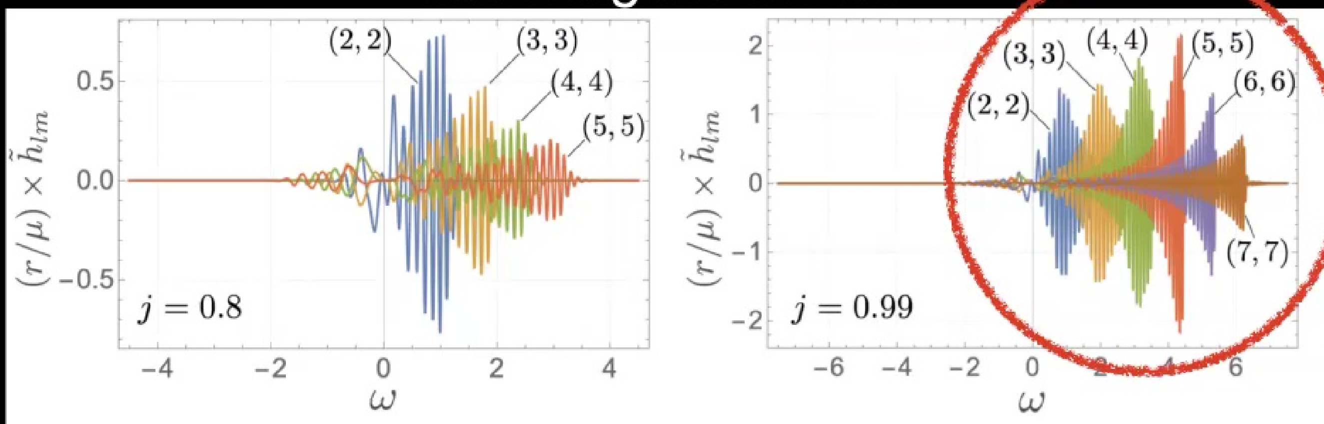

Slowly decaying QNMs

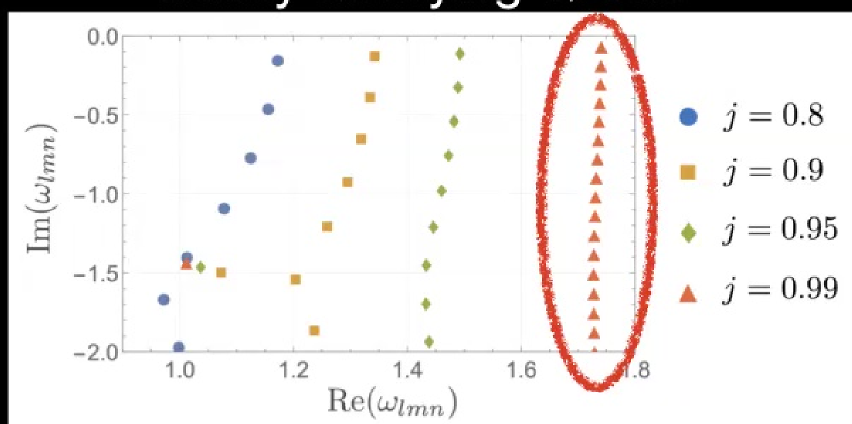

Measurement of the QN damping time and frequency by LISA

NO and Daichi Tsuna (2022)

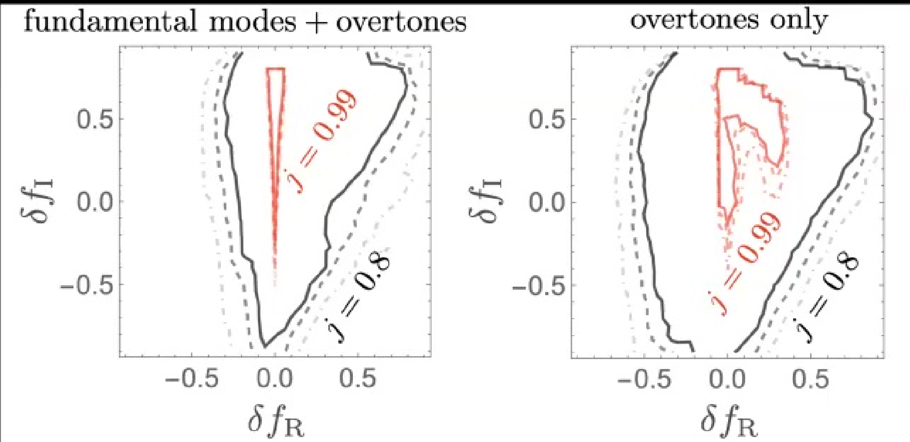

FIG. 5: Precision for measuring deviations of multiple QN modes from general relativity, for (left) $H_\delta^{(\rm F+O)}$ model with $(D_{\rm L}, \tilde{M}, q) = (3\ {\rm Gpc}, 10^7 M_\odot, 10^{-3})$ and (right) $H_\delta^{(\rm O)}$ model with $(1\ {\rm Gpc}, 10^7 M_\odot, 10^{-3})$. Red and black colors show spins of $j = 0.99$ and 0.8 respectively. Outside the solid, dashed and dot-dashed contours, the Bayes factor $\mathcal{B}$ takes values of > 3.2, > 10, and > 100, respectively.

$$\mathrm{Re}(\omega_{lmn}) = (1 + \delta f_{\rm R}) \times \mathrm{Re}(\omega_{lmn}^{(\rm GR)})$$

$$\mathrm{Im}(\omega_{lmn}) = (1 + \delta f_{\rm I}) \times \mathrm{Im}(\omega_{lmn}^{(\rm GR)})$$

GW data (numerical computation)

QNM model (GR)

$$\mathcal{B} = \frac{p(\tilde{h}|H_0)}{p(\tilde{h}|H_\delta)}$$

QNM model (modified)

$$p(d|H(\vec{\vartheta})) \propto \exp\left[-\frac{1}{2}\langle d - H(\vec{\vartheta}), d - H(\vec{\vartheta})\rangle\right]$$

$$\langle x, y\rangle \equiv 4\mathrm{Re}\int_0^\infty \frac{x(f)y^*(f)}{S_n} df$$

Difficulty in the measurement of the damping time

GW150914

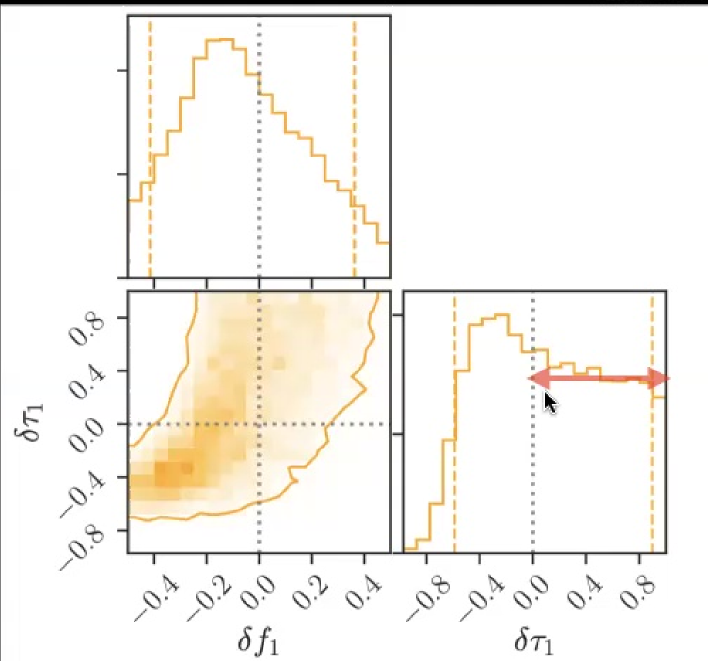

FIG. 4. Measurement of the frequency and damping time of the first overtone, using data starting at the peak. The colormap represents the posterior distribution of the fractional deviations δf_1 and $\delta\tau_1$ away from the no-hair value $\delta f_1 = \delta\tau_1 = 0$ (gray dotted lines). The solid contour and dashed vertical lines enclose 90% of the posterior probability. All other parameters, including M_f and χ_f have been marginalized away. Fixing $\delta f_1 = \delta\tau_1 = 0$ recovers the $N = 1$ analysis in Figs. 1 and 3.

M. Isi et al. (2019)

frequency of the first overtone

$$f_{221} = (1 + \delta f_1) \times f_{221}^{(\mathrm{GR})}$$

decay time of the first overtone

$$\tau_{221} = (1 + \delta\tau_1) \times \tau_{221}^{(\mathrm{GR})}$$

inferred peak of the strain. Fig. 4 shows the resulting marginalized posterior over the fractional frequency and damping time deviations (δf_1 and $\delta\tau_1$ respectively). With 68% credibility, we measure $\delta f_1 = -0.05 \pm 0.2$. To that level of credibility, this establishes agreement with the no-hair hypothesis ($\delta f_1 = 0$) at the 20% level. The damping time is largely unconstrained in the $-0.06 \lesssim \delta\tau_1 \lesssim 1$ range. This has little impact on the frequency measurement, which is unaffected by setting $\delta\tau_1 = 0$. We find that the ratio of marginal likelihoods (the Bayes factor) between the no-hair model ($\delta f_1 = \delta\tau_1 = 0$) and our floating frequency and damping time model is 1.75.

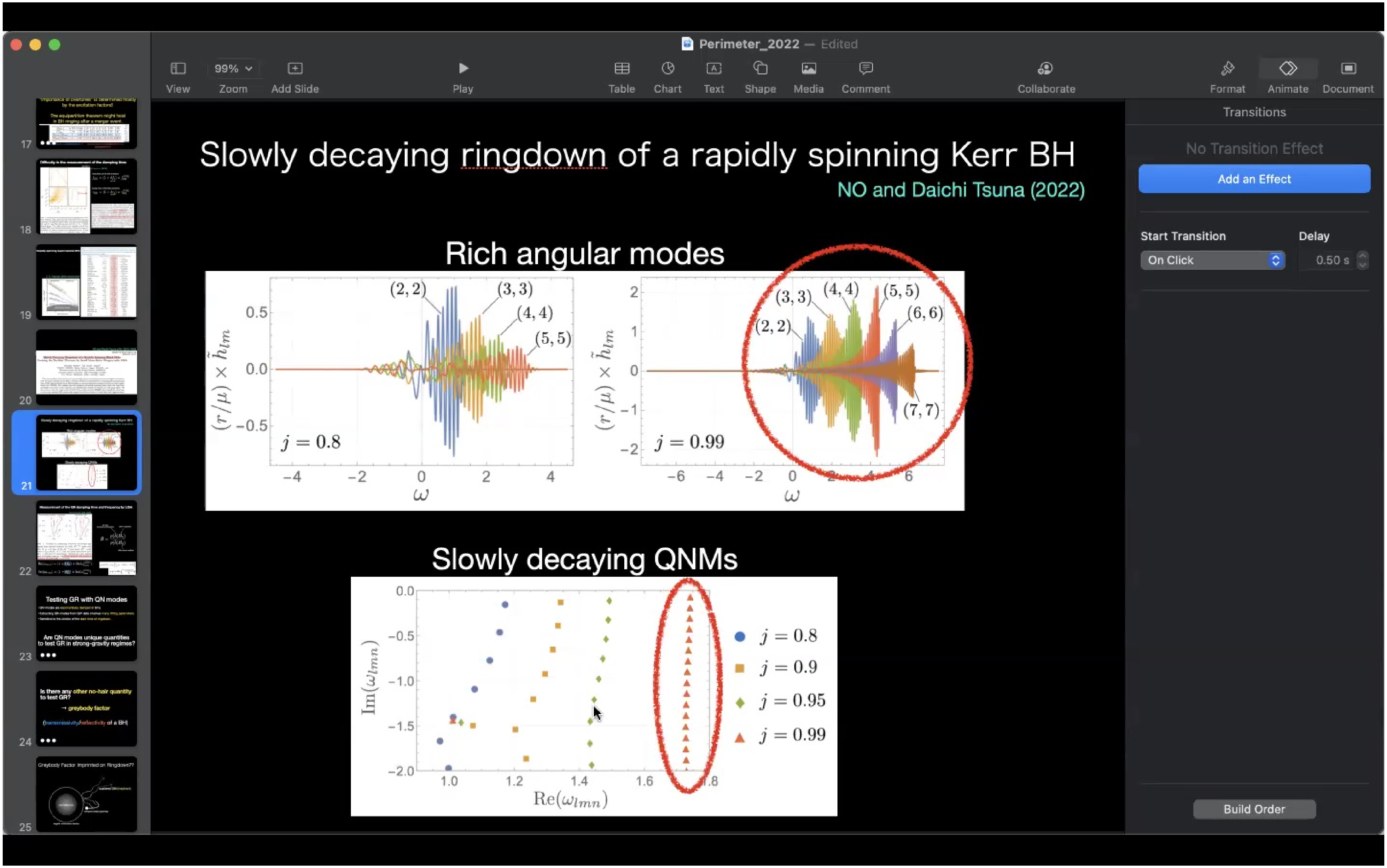
Perimeter_2022 — Edited
Slowly decaying ringdown of a rapidly spinning Kerr BH
NO and Daichi Tsuna (2022)
Rich angular modes
$(r/\mu)\times\tilde{h}_{lm}$
$j=0.8$
$j=0.99$
(2, 2) (3, 3) (4, 4) (5, 5) (6, 6) (7, 7)
ω
Slowly decaying QNMs
$\mathrm{Im}(\omega_{lmn})$
$\mathrm{Re}(\omega_{lmn})$
$j=0.8$
$j=0.9$
$j=0.95$
$j=0.99$
Transitions
No Transition Effect
Add an Effect
Start Transition
On Click
Delay
0.50 s
Build Order

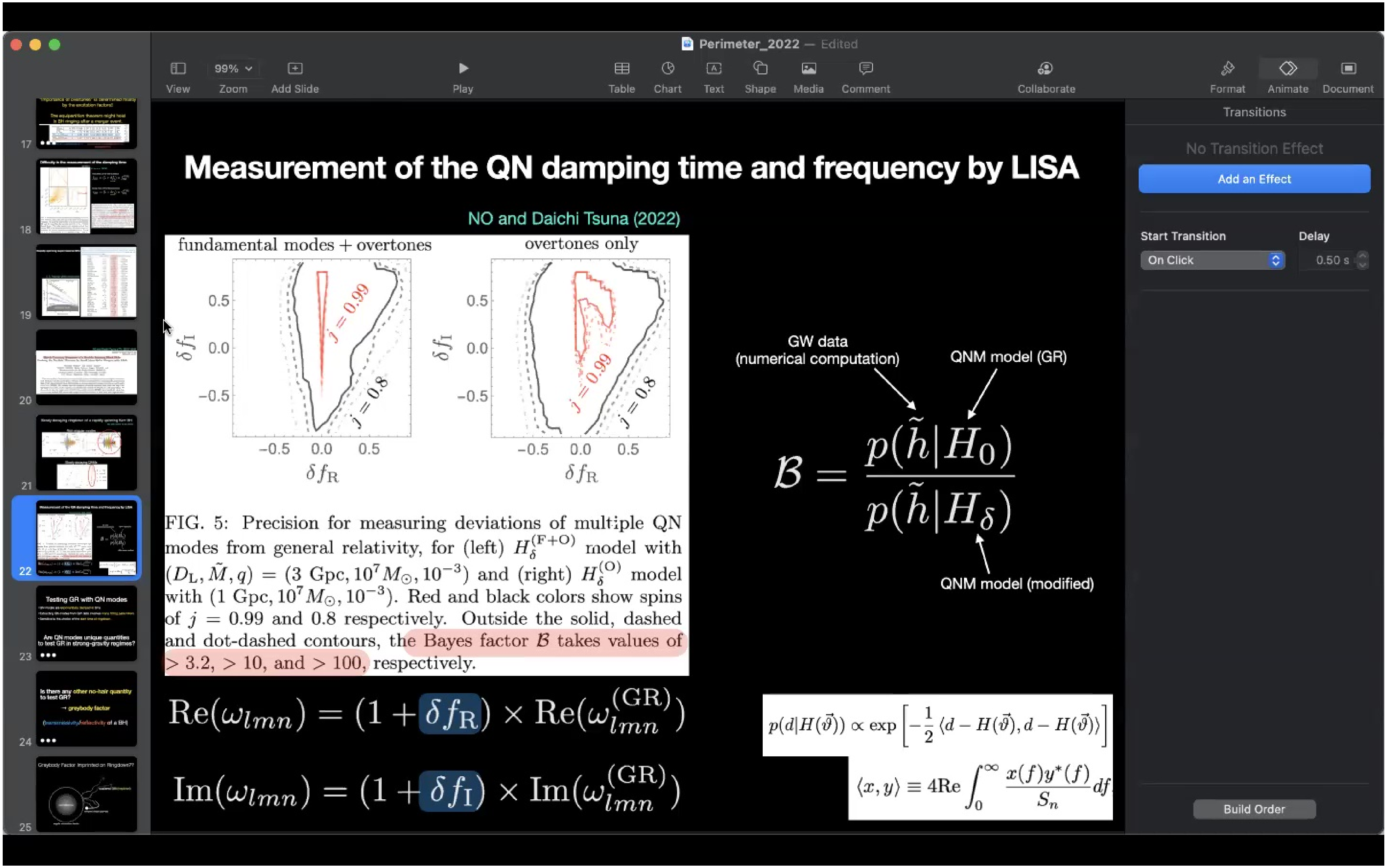
Perimeter_2022 — Edited
Measurement of the QN damping time and frequency by LISA
NO and Daichi Tsuna (2022)
fundamental modes + overtones
overtones only
$j = 0.99$
$j = 0.8$
$\delta f_{\rm I}$
$\delta f_{\rm R}$
FIG. 5: Precision for measuring deviations of multiple QN modes from general relativity, for (left) $H_\delta^{\rm (F+O)}$ model with $(D_{\rm L}, \tilde{M}, q) = (3\ {\rm Gpc}, 10^7 M_\odot, 10^{-3})$ and (right) $H_\delta^{\rm (O)}$ model with $(1\ {\rm Gpc}, 10^7 M_\odot, 10^{-3})$. Red and black colors show spins of $j = 0.99$ and 0.8 respectively. Outside the solid, dashed and dot-dashed contours, the Bayes factor $\mathcal{B}$ takes values of > 3.2, > 10, and > 100, respectively.
GW data (numerical computation)
QNM model (GR)
QNM model (modified)
$\mathcal{B} = \frac{p(\tilde{h}|H_0)}{p(\tilde{h}|H_\delta)}$
${\rm Re}(\omega_{lmn}) = (1 + \delta f_{\rm R}) \times {\rm Re}(\omega_{lmn}^{\rm (GR)})$
${\rm Im}(\omega_{lmn}) = (1 + \delta f_{\rm I}) \times {\rm Im}(\omega_{lmn}^{\rm (GR)})$
$p(d|H(\vec{\vartheta})) \propto \exp\left[-\frac{1}{2}\langle d - H(\vec{\vartheta}), d - H(\vec{\vartheta})\rangle\right]$
$\langle x, y\rangle \equiv 4{\rm Re}\int_0^\infty \frac{x(f)y^*(f)}{S_n} df$
Transitions
No Transition Effect
Add an Effect
Start Transition
On Click
Delay
0.50 s
Build Order

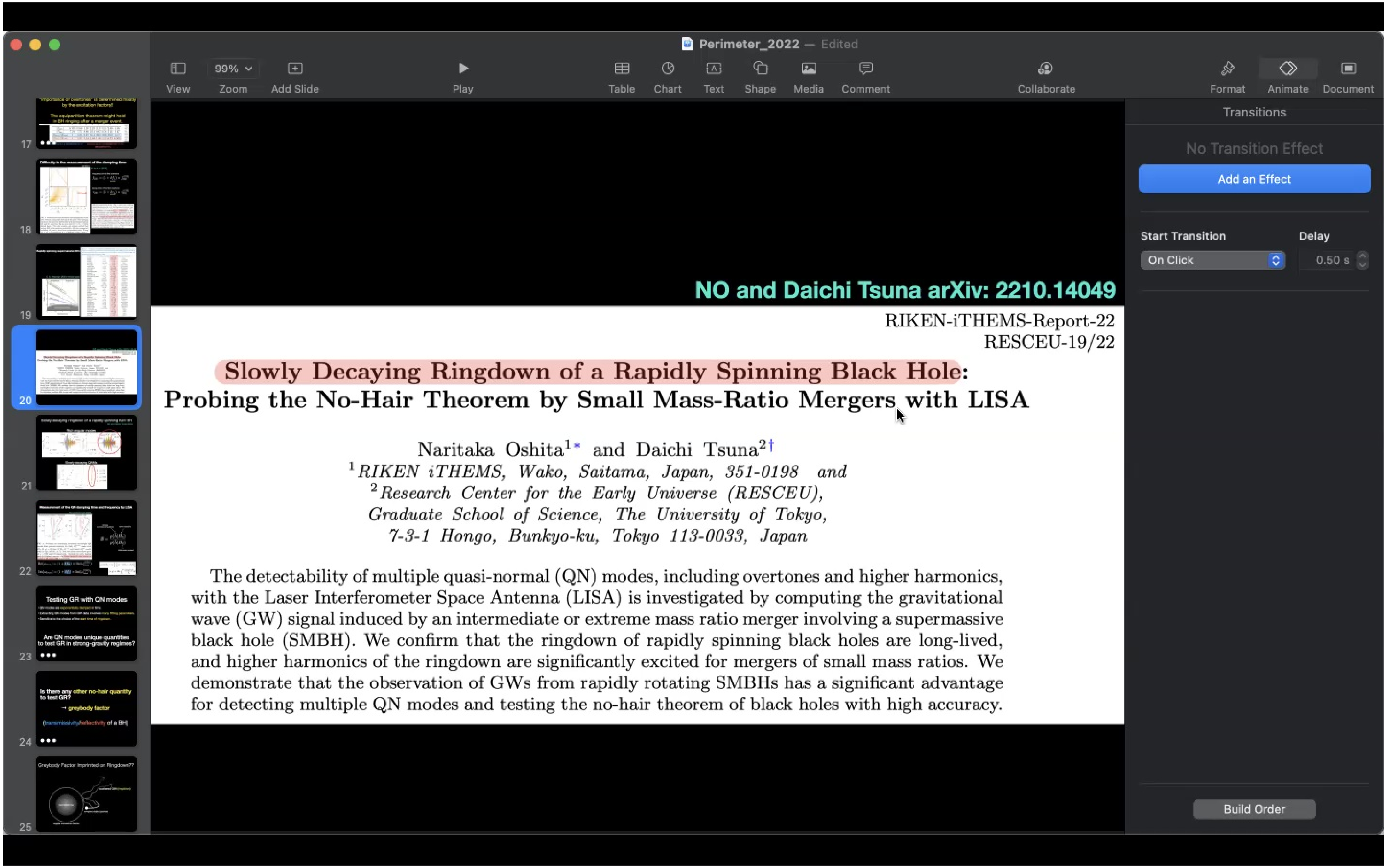
NO and Daichi Tsuna arXiv: 2210.14049

RIKEN-iTHEMS-Report-22
RESCEU-19/22

Slowly Decaying Ringdown of a Rapidly Spinning Black Hole: Probing the No-Hair Theorem by Small Mass-Ratio Mergers with LISA

Naritaka Oshita[1*] and Daichi Tsuna[2†]

[1] *RIKEN iTHEMS, Wako, Saitama, Japan, 351-0198 and*
[2] *Research Center for the Early Universe (RESCEU), Graduate School of Science, The University of Tokyo, 7-3-1 Hongo, Bunkyo-ku, Tokyo 113-0033, Japan*

The detectability of multiple quasi-normal (QN) modes, including overtones and higher harmonics, with the Laser Interferometer Space Antenna (LISA) is investigated by computing the gravitational wave (GW) signal induced by an intermediate or extreme mass ratio merger involving a supermassive black hole (SMBH). We confirm that the ringdown of rapidly spinning black holes are long-lived, and higher harmonics of the ringdown are significantly excited for mergers of small mass ratios. We demonstrate that the observation of GWs from rapidly rotating SMBHs has a significant advantage for detecting multiple QN modes and testing the no-hair theorem of black holes with high accuracy.

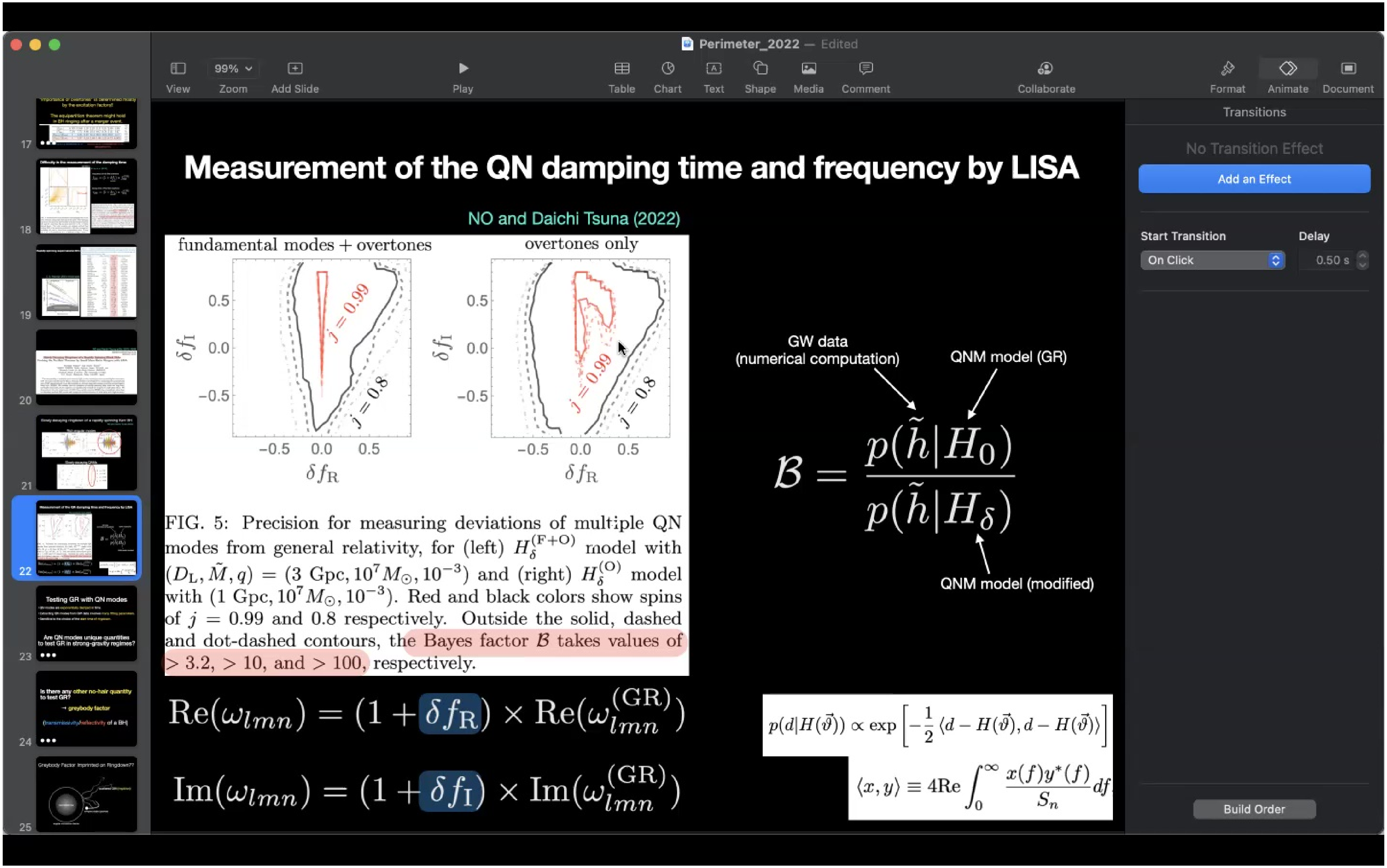
Perimeter_2022 — Edited
Measurement of the QN damping time and frequency by LISA
NO and Daichi Tsuna (2022)
fundamental modes + overtones
overtones only
$j = 0.99$
$j = 0.8$
$\delta f_{\rm I}$
$\delta f_{\rm R}$
FIG. 5: Precision for measuring deviations of multiple QN modes from general relativity, for (left) $H_\delta^{(\rm F+O)}$ model with $(D_{\rm L}, \tilde{M}, q) = (3\ {\rm Gpc}, 10^7 M_\odot, 10^{-3})$ and (right) $H_\delta^{(\rm O)}$ model with $(1\ {\rm Gpc}, 10^7 M_\odot, 10^{-3})$. Red and black colors show spins of $j = 0.99$ and 0.8 respectively. Outside the solid, dashed and dot-dashed contours, the Bayes factor $\mathcal{B}$ takes values of > 3.2, > 10, and > 100, respectively.
GW data
(numerical computation)
QNM model (GR)
QNM model (modified)
$\mathcal{B} = \frac{p(\tilde{h}|H_0)}{p(\tilde{h}|H_\delta)}$
${\rm Re}(\omega_{lmn}) = (1 + \delta f_{\rm R}) \times {\rm Re}(\omega_{lmn}^{(\rm GR)})$
${\rm Im}(\omega_{lmn}) = (1 + \delta f_{\rm I}) \times {\rm Im}(\omega_{lmn}^{(\rm GR)})$
$p(d|H(\vec{\vartheta})) \propto \exp\left[-\frac{1}{2}\langle d - H(\vec{\vartheta}), d - H(\vec{\vartheta})\rangle\right]$
$\langle x, y\rangle \equiv 4{\rm Re}\int_0^\infty \frac{x(f)y^*(f)}{S_n} df$

Testing GR with QN modes

- QN modes are exponentially damped in time.
- Extracting QN modes from GW data involves many fitting parameters.
- Sensitive to the choice of the start time of ringdown.

Testing GR with QN modes

- QN modes are exponentially damped in time.
- Extracting QN modes from GW data involves many fitting parameters.
- Sensitive to the choice of the start time of ringdown.

Are QN modes unique quantities to test GR in strong-gravity regimes?

Is there any other no-hair quantity to test GR?

→ greybody factor

(transmissivity/reflectivity of a BH)

GW waveform induced by a particle plunging into a BH

Extreme-Mass-Ratio Merger

Y. Kojima and T. Nakamura (1984)

Sasaki Nakamura equation

$$\left(\frac{d^2}{dr^{*2}} - F_{lm}\frac{d}{dr^*} - U_{lm}\right) X_{lm} = T_{lm}$$

Trajectory
(solving the geodesic equation and *NO self-force*)

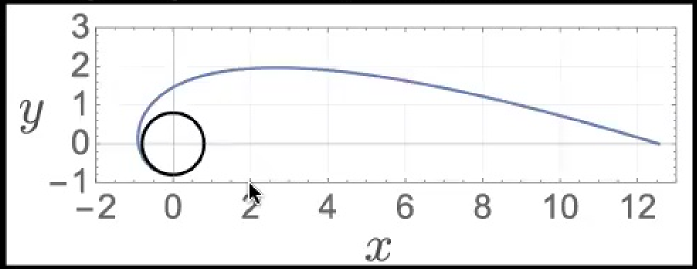

Signal (spectrum)

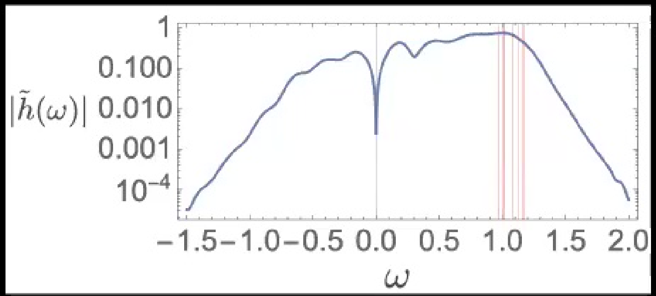

GW waveform induced by a particle plunging into a BH

Extreme-Mass-Ratio Merger

Y. Kojima and T. Nakamura (1984)

Sasaki Nakamura equation

$$\left(\frac{d^2}{dr^{*2}} - F_{lm}\frac{d}{dr^*} - U_{lm}\right) X_{lm} = T_{lm}$$

Trajectory
(solving the geodesic equation and *NO self-force*)

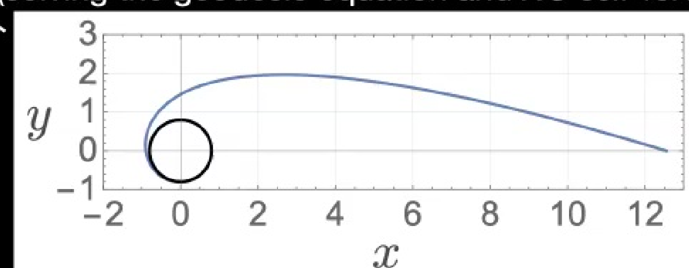

Signal (spectrum)

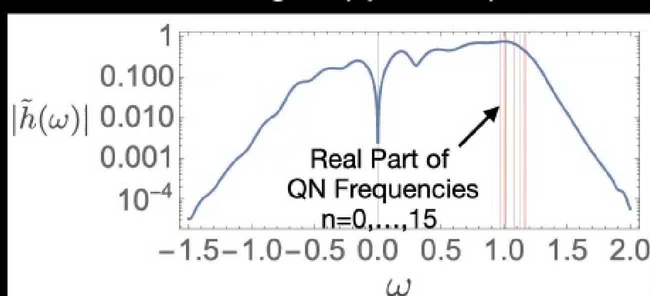

Inverse
Fourier Transform

Signal (time domain)

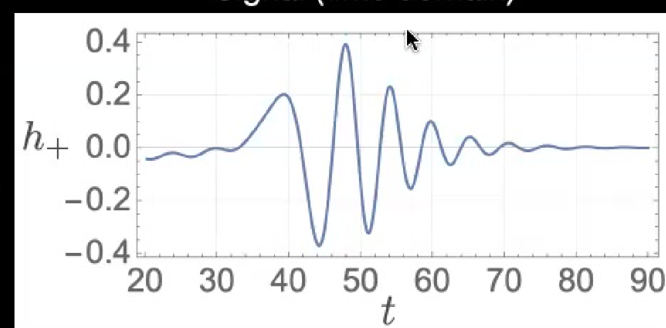

Exponential cut-off in frequency domain

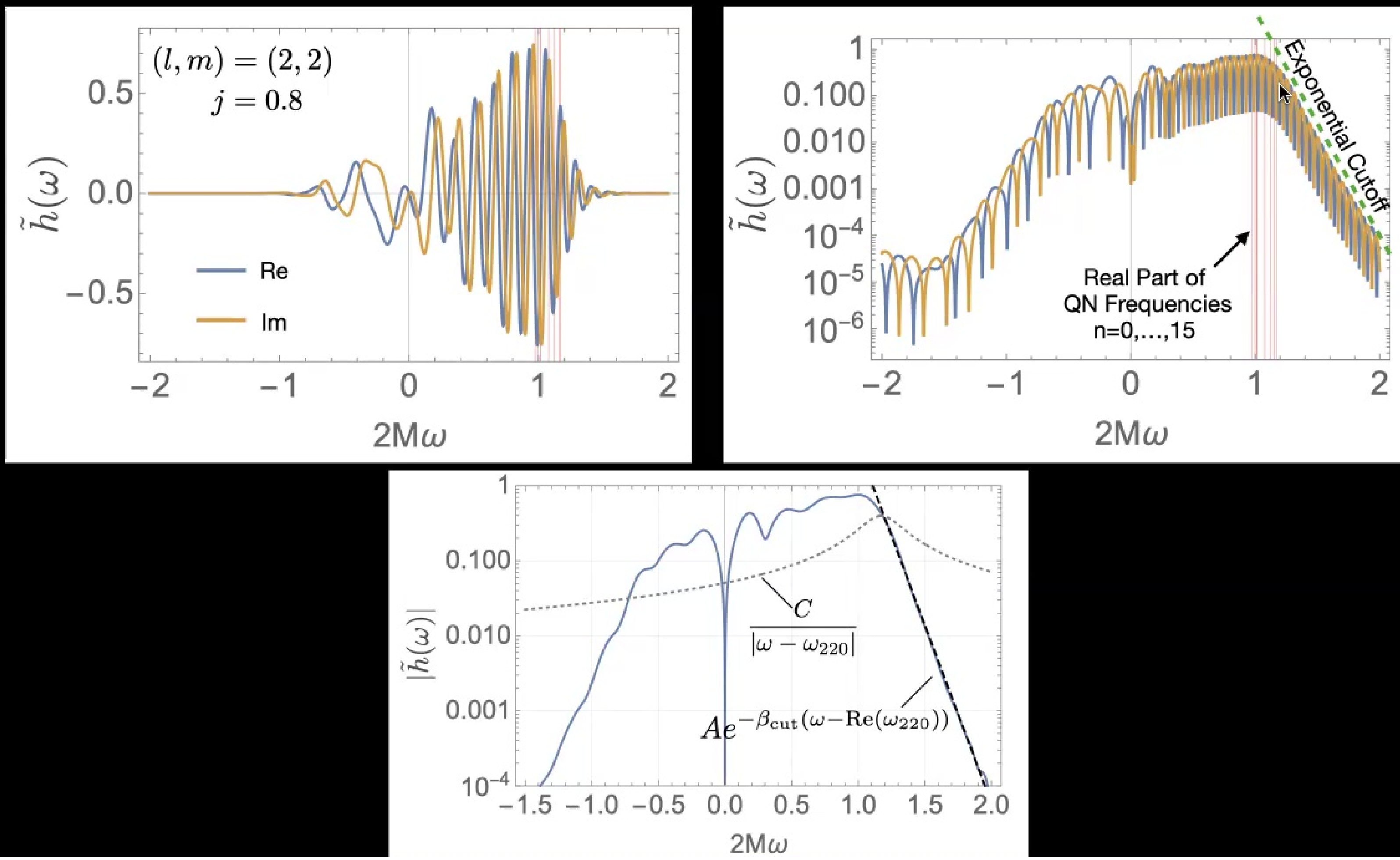

Fermi-Dirac statistics and Kerr Ringdown

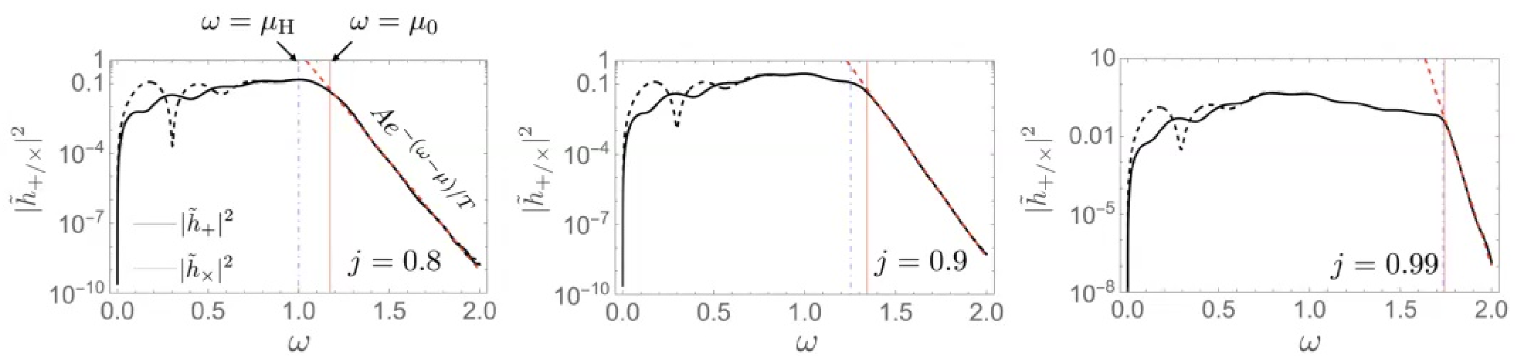

FIG. 8: The absolute square of the spectral amplitude of the GW signals for $j = 0.8$, $j = 0.9$, and $j = 0.99$ with $l = m = 2$. The Boltzmann distribution (fitted with the red dashed line) appears at higher frequencies than $\omega = \mu_0$ (red solid line). The blue dot-dashed line indicates $\omega = \mu_{\rm H}$.

NO (2022)

$$2M = 1 \quad (l, m) = (2, 2)$$

$\mu_{\rm H} = m\Omega_{\rm H}$ superradiant frequency

$\mu_0 = {\rm Re}(\omega_{lm0})$ fundamental QN frequency

$$\frac{1}{e^{(\omega-\mu)/T} + 1}$$

Fermi-Dirac distribution ?

Fermi-Dirac statistics and Kerr Ringdown

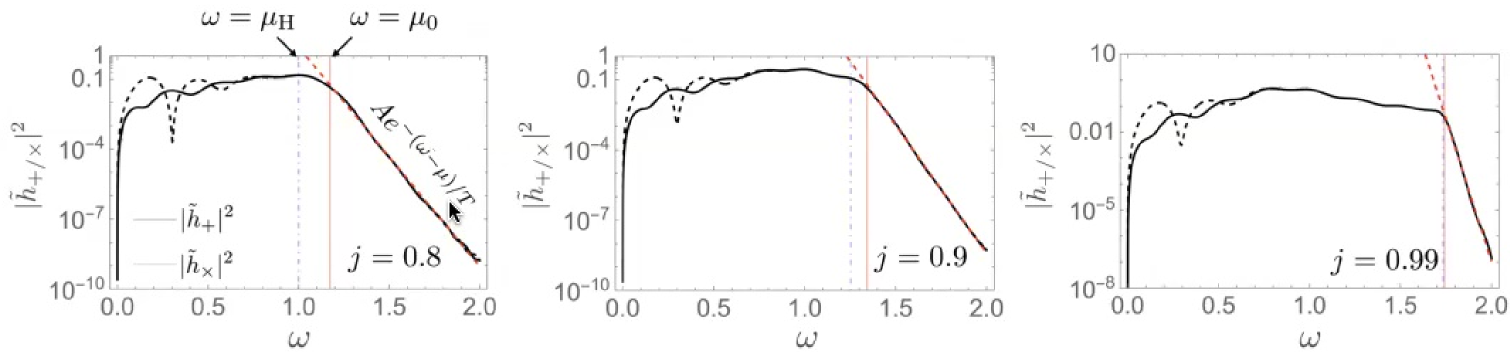

FIG. 8: The absolute square of the spectral amplitude of the GW signals for $j = 0.8$, $j = 0.9$, and $j = 0.99$ with $l = m = 2$. The Boltzmann distribution (fitted with the red dashed line) appears at higher frequencies than $\omega = \mu_0$ (red solid line). The blue dot-dashed line indicates $\omega = \mu_H$.

NO (2022)

$2M = 1 \quad (l, m) = (2, 2)$

$\mu_H = m\Omega_H$ superradiant frequency

$\mu_0 = \mathrm{Re}(\omega_{lm0})$ fundamental QN frequency

$$\frac{1}{e^{(\omega-\mu)/T} + 1}$$

Fermi-Dirac distribution ?

T → obtained by fitting analysis

Fitting the Boltzmann factor to GW data

$$\frac{1}{e^{(\omega-\mu)/T}+1} \sim e^{-(\omega-\mu)/T}$$

"Boltzmann" at higher frequencies

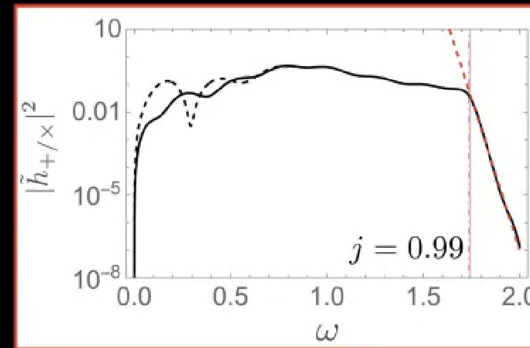

NO (2022)

(l,m)	$j=0.8$ ($T_{\rm H} \simeq 0.0597$)			$j=0.9$ ($T_{\rm H} \simeq 0.0483$)			$j=0.99$ ($T_{\rm H} \simeq 0.0197$)		
	T	[redacted]	[redacted]	T	[redacted]	[redacted]	T	[redacted]	[redacted]
$(2,2)$	0.0462(2)	[redacted]	[redacted]	0.0397(2)	[redacted]	[redacted]	0.0198(2)	[redacted]	[redacted]
$(3,3)$	0.0493(2)	[redacted]	[redacted]	0.0375(1)	[redacted]	[redacted]	0.0196(3)	[redacted]	[redacted]
$(4,4)$	0.0565(1)	[redacted]	[redacted]	0.0454(2)	[redacted]	[redacted]	0.0200(3)	[redacted]	[redacted]
$(5,5)$	0.0552(2)	[redacted]	[redacted]	0.0483(1)	[redacted]	[redacted]	0.0196(4)	[redacted]	[redacted]

Relative Error

$$\Delta_0 \equiv |T - T_0|/T_0, \ \ \Delta_{\rm H} \equiv |T - T_{\rm H}|/T_{\rm H}$$

$$T_0 \equiv |{\rm Im}(\omega_{lm0})|/\pi$$

frequency defined by the fundamental QN damping time

$$T_{\rm H} \equiv \frac{\sqrt{1-j^2}}{4\pi r_+}$$

Hawking frequency

Greybody Factor Imprinted on Ringdown

NO (2022)

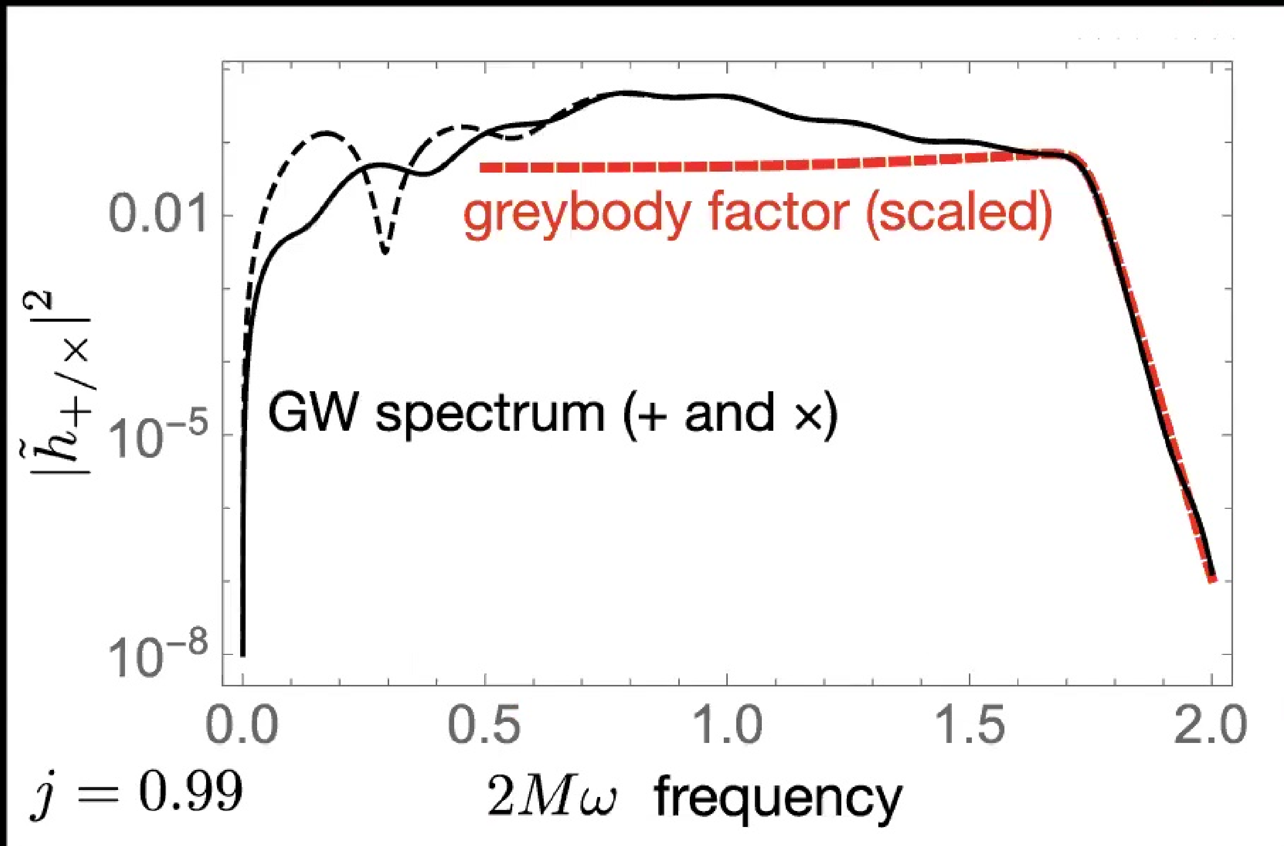

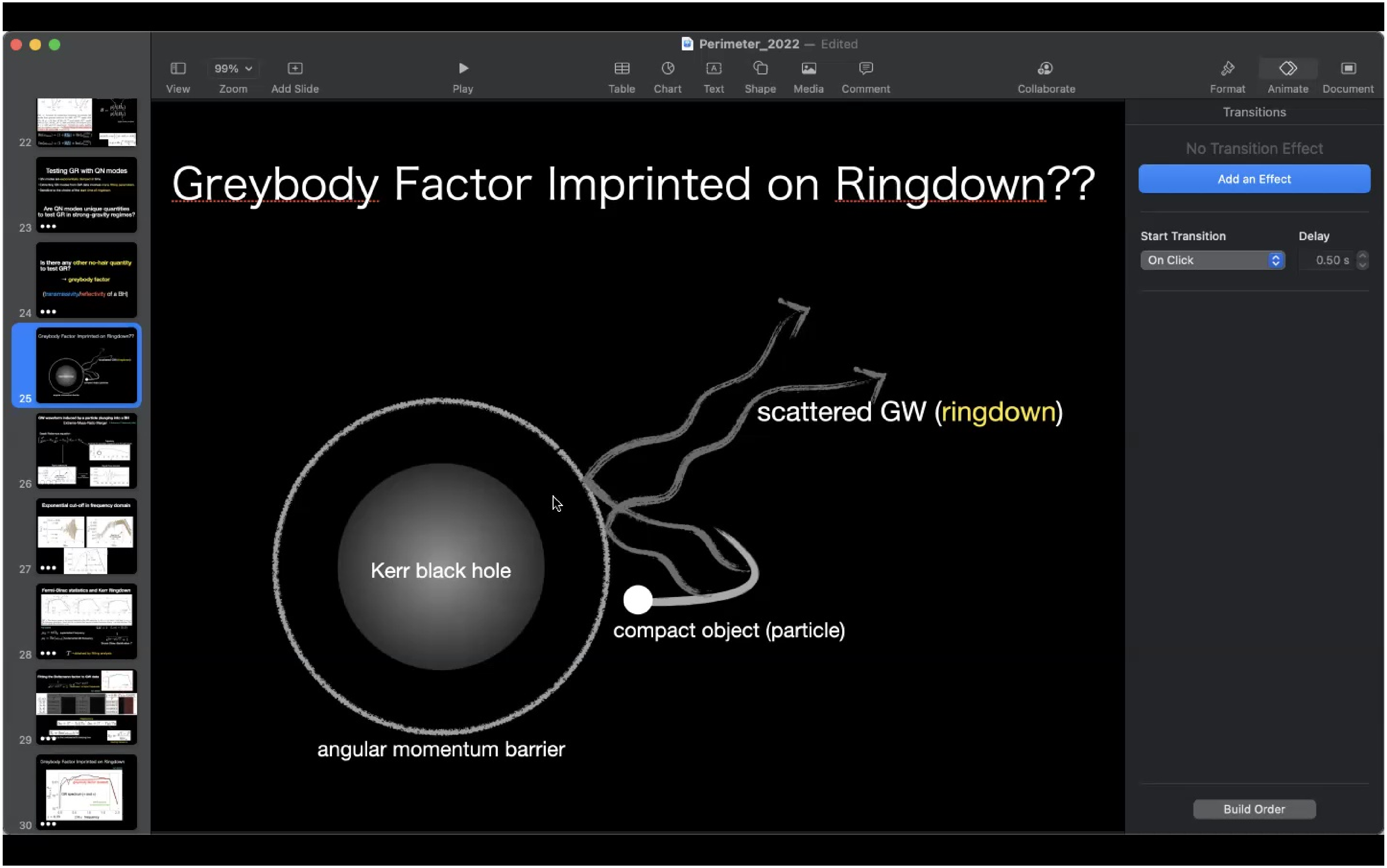

Perimeter_2022 — Edited
Greybody Factor Imprinted on Ringdown??
scattered GW (ringdown)
Kerr black hole
compact object (particle)
angular momentum barrier

reflectivity of a BH $\simeq$ Fermi-Dirac distribution

(WKB approximation) e.g. S. Iyer et al. (1987), R. A. Konoplya et al. (2019)

$$1-\Gamma_{lm} \simeq \frac{1}{1+e^{(\omega - m\Omega_{\rm H})/T}}$$

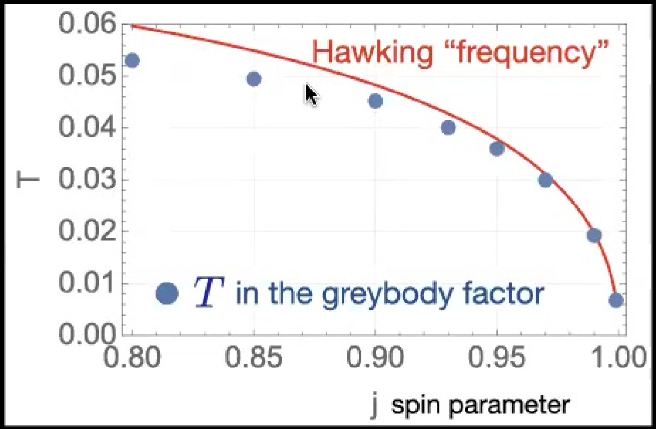

reflectivity of a BH $\simeq$ Fermi-Dirac distribution

(WKB approximation) e.g. S. Iyer et al. (1987), R. A. Konoplya et al. (2019)

$$1 - \Gamma_{lm} \simeq \frac{1}{1 + e^{(\omega - m\Omega_{\rm H})/T}}$$

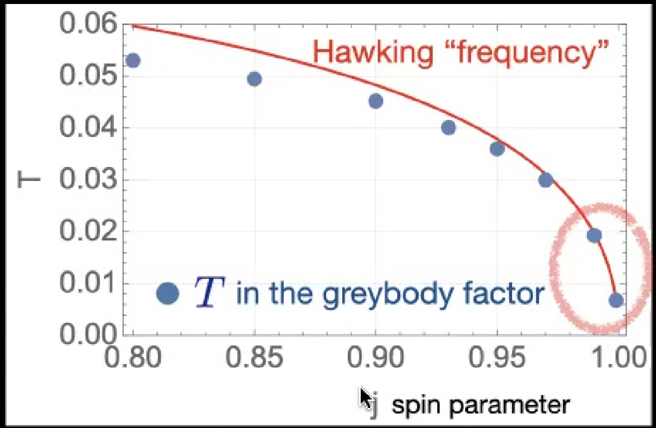

$$(\text{Hawking temperature}) = (\hbar/k_{\rm B})(\text{Hawking frequency})$$

Quantum *Classical*

apparent thermal ringdown
from an extreme-mass-ratio merger

Fermi degeneracy of Kerr ringdown

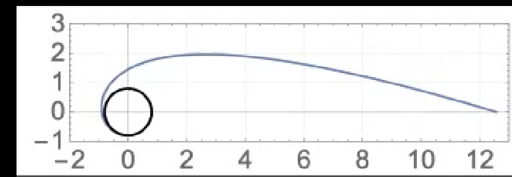

j=0.99 (low Hawking temperature) $T_{\rm H} = \frac{\sqrt{1-j^2}}{4\pi r_+}$ $\Omega_{\rm H} = \frac{j}{2r_+}$

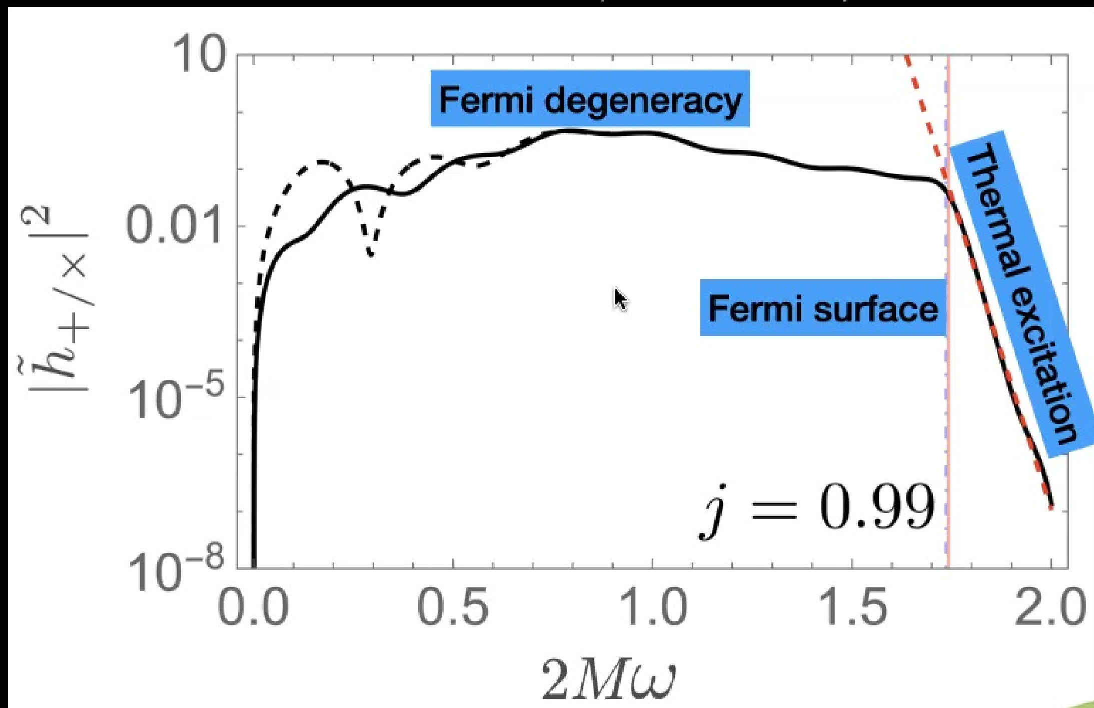

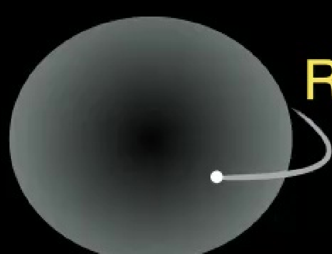

Ringdown of a near-extremal BH
→ Thermal Fermi system??

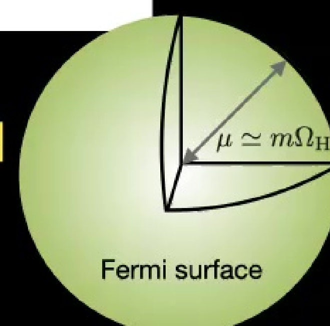

QN modes ~ Matsubara modes

S. Hod, (2008), H. Yang, et al. (2013)

Kerr QN frequencies for j~1

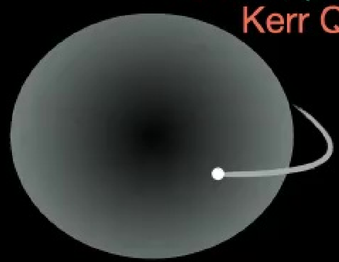

$$\omega \simeq \mu_{\rm H} - i\left(\frac{1}{2}+n\right)2\pi T_{\rm H}$$

Matsubara frequencies

$$\frac{1}{e^{(\omega-\mu_{\rm H})/T_{\rm H}}+1}$$

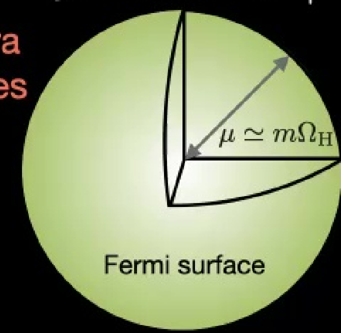

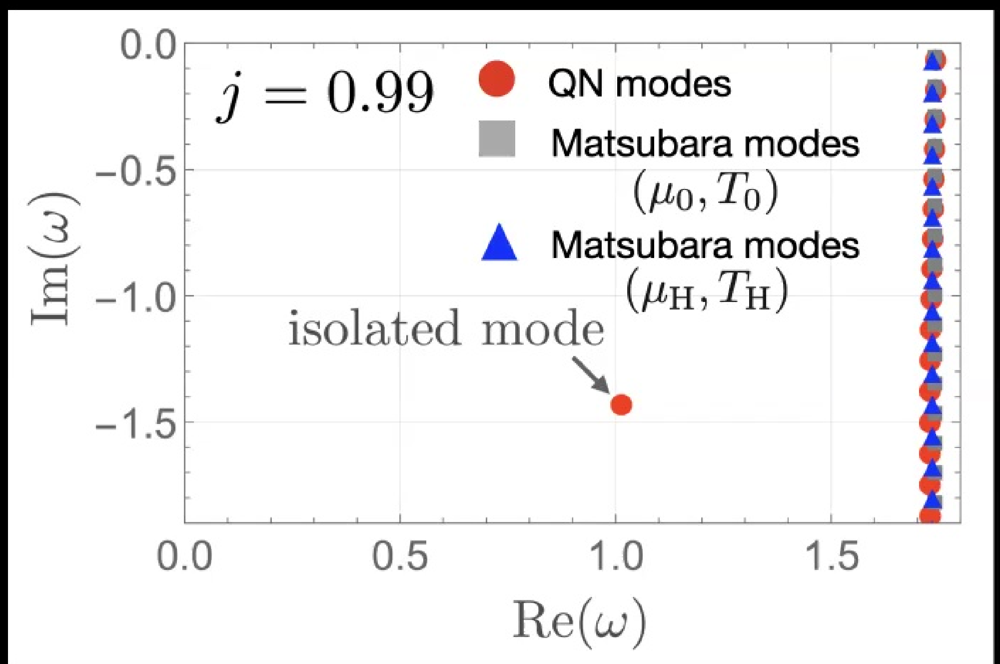

Summary

Excitation of overtones

Excitability of QN modes is quantified by the “excitation factor”

It has the peak around at n=5.

↑

Consistent with the result of numerical relativity!!

Greybody Factor can be measurable by Ringdown Observation
(Ringdown of an extreme-mass-ratio merger)

exponential cutoff in the ringdown spectrum
→ Boltzmann factor with ~ Hawking frequency

near-extremal BH -> Fermi surface at $\omega = m\Omega_{\rm H}$

QN modes ~ Matsubara modes
in the near-extremal limit

Excitation factors

N.O. arXiv: 2109.09757

E_{lmn}

$l = m = 2$

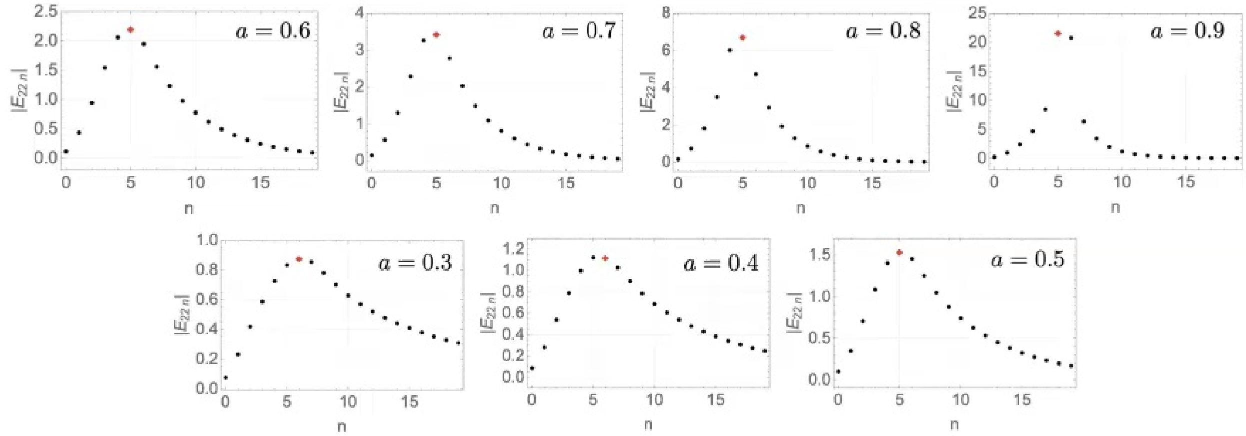

FIG. 1: The QNEFs for $a = 0.3$, 0.4, 0.5, 0.6, 0.7, 0.8, and 0.9 with $l = m = 2$. The maximum value of QNEF is indicated by red points.

QN frequencies

$\mathrm{Re}(\omega_{lmn})$

$l = m = 2$

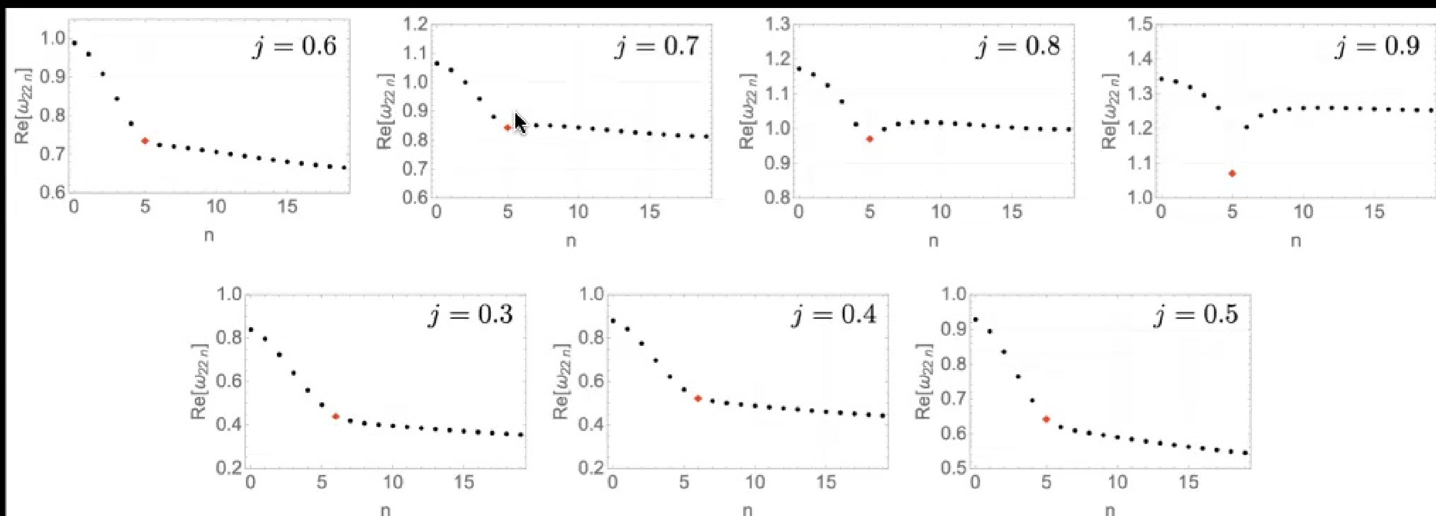

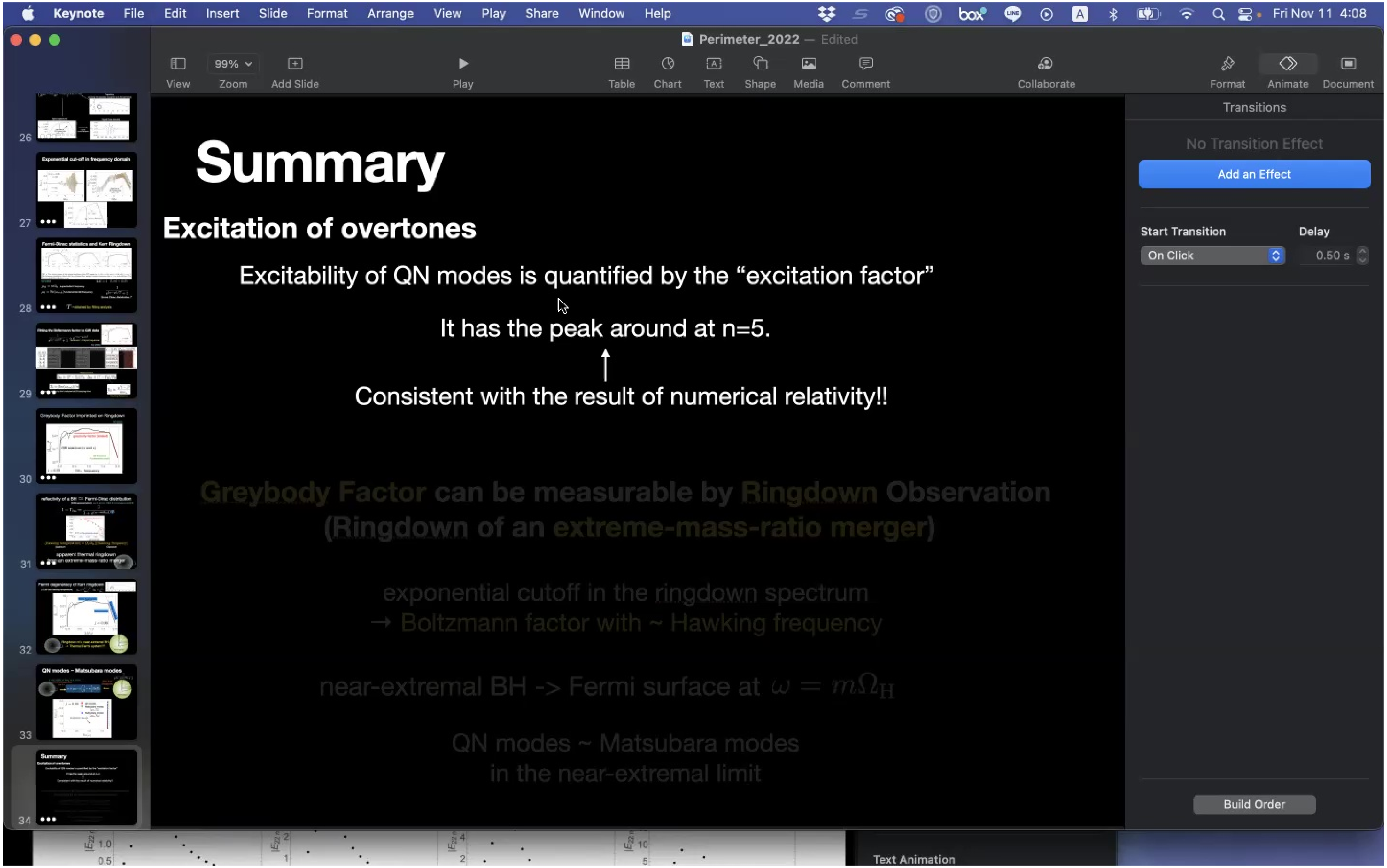
Perimeter_2022 — Edited
Summary
Excitation of overtones
Excitability of QN modes is quantified by the “excitation factor”
It has the peak around at n=5.
Consistent with the result of numerical relativity!!
Greybody Factor can be measurable by Ringdown Observation
(Ringdown of an extreme-mass-ratio merger)
exponential cutoff in the ringdown spectrum
→ Boltzmann factor with ~ Hawking frequency
near-extremal BH -> Fermi surface at $\omega = m\Omega_{\rm H}$
QN modes ~ Matsubara modes
in the near-extremal limit
Transitions
No Transition Effect
Add an Effect
Start Transition
On Click
Delay
0.50 s
Build Order
Text Animation